

# NV-Metamaterial: Tunable Quantum Hyperbolic Metamaterial Using Nitrogen-Vacancy Centers in Diamond

Qing Ai,<sup>1,2</sup> Peng-Bo Li,<sup>1,3</sup> Wei Qin,<sup>1,4</sup> C. P. Sun,<sup>5</sup> and Franco Nori<sup>1,6</sup>

<sup>1</sup>*CEMS, RIKEN, Wako-shi, Saitama 351-0198, Japan*

<sup>2</sup>*Department of Physics, Applied Optics Beijing Area Major Laboratory, Beijing Normal University, Beijing 100875, China*

<sup>3</sup>*Department of Applied Physics, Xi'an Jiaotong University, Xi'an 710049, China*

<sup>4</sup>*Quantum Physics and Quantum Information Division, Beijing Computational Science Research Center, Beijing 100193, China*

<sup>5</sup>*Beijing Computational Science Research Center & Graduate School of Chinese Academy of Engineering Physics, Beijing 100084, China*

<sup>6</sup>*Department of Physics, The University of Michigan, Ann Arbor, Michigan 48109-1040, USA*

We show that nitrogen-vacancy (NV) centers in diamond can produce a novel quantum hyperbolic metamaterial. We demonstrate that a hyperbolic dispersion relation in diamond with NV centers can be engineered and dynamically tuned by applying a magnetic field. This quantum hyperbolic metamaterial with a tunable window for the negative refraction allows for the construction of a superlens beyond the diffraction limit. In addition to subwavelength imaging, this NV-metamaterial can be used in spontaneous emission enhancement, heat transport and acoustics, analogue cosmology, and lifetime engineering. Therefore, our proposal interlinks the two hotspot fields, i.e., NV centers and metamaterials.

*Metamaterials.*—Metamaterials with negative refraction have attracted broad interest [1–4]. Metamaterials can be used, e.g., for electromagnetic cloaking, perfect lens beyond diffraction limit [2], fingerprint identification in forensic science [5], simulating condensate matter phenomena [6] and reversed Doppler effect [7]. In order to realize negative refraction, sophisticated composite architectures [3, 8] and topologies [9–12] are fabricated to achieve simultaneously negative permittivity and permeability. However, hyperbolic (or indefinite) metamaterials were proposed [13–15, 19] to overcome the difficulty of inducing a magnetic transition at the same frequency as the electric response. The magnetic response of double-negative metamaterials is so weak that it effectively shortens the frequency window of the negative refraction [9]. In addition to subwavelength imaging [17, 18] and focusing [18], hyperbolic metamaterials have been used to realize spontaneous emission enhancement [19], applied in heat transport [20] and acoustics [21], analogue cosmology [22], and lifetime engineering [23, 24].

*NV centers.*—On the other hand, quantum devices based on nitrogen-vacancy (NV) centers in diamond are under intense investigation [25, 26] as they manifest some novel properties and can be explored for many interesting applications [1, 28]. For example, NV centers in diamond have been proposed to realize a laser [29] and maser [30] at room temperature. Highly-sensitive solid-state gyroscopes [31] based on ensembles of NV centers in diamond can be realized by dynamical decoupling, to suppress the dipolar relaxation. Shortcuts to adiabaticity have been successfully performed in NV centers of diamond to initialize and transfer coherent superpositions [32, 33]. The high sensitivity to external signals makes single NV centers promising for quantum sensing of various physical parameters, such as electric field [34, 35], magnetic field [36–38], single electron and nuclear spin [39–46], and temperature [47–49]. Numerous hybrid quantum devices, composed of NV centers and other quantum systems, e.g. superconducting circuits and carbon nanotubes, have been proposed to realize demanding tasks [50–54].

*NV-metamaterials.*—Inspired by the rapid progress in both fields, here we propose to realize a hyperbolic metamaterial using NV centers in diamond. We consider an electric hyperbolic metamaterial, in which two principal components of its electric permittivity possess different signs. When an optical electromagnetic field induces the transition  ${}^3A_2 \rightleftharpoons {}^3E$ , the NV centers in diamond will negatively respond to the electric field in one direction. This process effectively modifies the relative permittivity of the diamond with NV centers and thus one principal component has a different sign. When a transverse magnetic (TH) mode is incident on this diamond with the principal axis of the negative component perpendicular to the interface, the transmitted light will be negatively refracted, as both the incident and transmitted light lie at the same side of the normal to the interface. Note that it is difficult to fabricate classical metamaterials working in the optical-frequency domain, because the sizes of the elements therein are sub-micron. However, the NV centers in diamond can be easily fabricated in several ways [1], e.g., as an in-grown product of the chemical vapour deposition diamond synthesis process, as a product of radiation damage and annealing, as well as ion implantation and annealing in bulk and nanocrystalline diamond. The NV-metamaterials proposed here solve this problem.

*Model.*—As schematically illustrated in Fig. 1(a), an NV center is composed of a vacancy, e.g. site O, and a

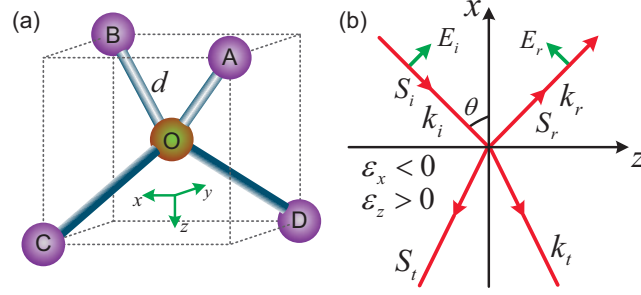


Figure 1. (color online) (a) Four possible orientations of NV centers in diamond [1, 14]:  $\vec{r}_{OA} = (-1, -1, -1)/\sqrt{3}$ ,  $\vec{r}_{OB} = (1, 1, -1)/\sqrt{3}$ ,  $\vec{r}_{OC} = (1, -1, 1)/\sqrt{3}$ ,  $\vec{r}_{OD} = (-1, 1, 1)/\sqrt{3}$ .  $d = 154$  pm is the length of carbon bond. The angle between any pair of the above four orientations is identically  $\alpha = 109^\circ 28'$ . (b) Negative refraction for hyperbolic dispersion with  $\epsilon_x < 0$  and  $\epsilon_z > 0$ . The TH mode is incident on the  $yz$  interface with electric field  $\vec{E}_i$ , wavevector  $\vec{k}_i$ , and Poynting vector  $\vec{S}_i$ . The angle between the normal ( $x$ -axis) and the incident field is  $\theta$ . It is reflected with electric field  $\vec{E}_r$ , wavevector  $\vec{k}_r$ , and Poynting vector  $\vec{S}_r$ . The Poynting and wavevector of the transmitted wave are, respectively,  $\vec{S}_t$  and  $\vec{k}_t$ .

substitutional nitrogen atom at one of its four possible neighboring sites, e.g. site A, B, C and D. The electronic ground state is a spin-triplet state with Hamiltonian [1, 55]

$$H_{\text{gs}} = D_{\text{gs}} S_z^2 + \mu_B g_{\text{gs}}^{\parallel} B_z S_z + \mu_B g_{\text{gs}}^{\perp} (B_x S_x + B_y S_y), \quad (1)$$

where  $D_{\text{gs}} = 2.88$  GHz is the zero-field splitting of the electronic ground state,  $\mu_B$  is the Bohr magneton,  $g_{\text{gs}}^{\parallel} \simeq g_{\text{gs}}^{\perp} = g_{\text{gs}} \simeq 2$  are respectively the components of the  $g$ -factor of the electronic ground state,  $\vec{B}$  is the magnetic field, and  $S_{\alpha}$  ( $\alpha = x, y, z$ ) are the spin-1 operators for the electron spin.

At room temperature, when there is no electric and strain fields, the Hamiltonian of the electronic excited state is simplified as [1, 55]

$$H_{\text{es}} = D_{\text{es}}^{\parallel} S_z^2 + \mu_B g_{\text{es}}^{\text{RT}} \vec{B} \cdot \vec{S} + \xi (S_y^2 - S_x^2), \quad (2)$$

where  $D_{\text{es}}^{\parallel} = 1.42$  GHz is the zero-field splitting of the electronic excited state,  $g_{\text{es}}^{\text{RT}} \simeq 2.01$  is the  $g$ -factor of the electronic spin of the excited state at room temperature,  $\xi = 70$  MHz is the strain-related coupling.

As illustrated in Fig. 1(a), there are four possible orientations for the NV centers in diamond [1, 14, 25, 26, 28, 55]. Since both Hamiltonians of the ground and excited states are obviously dependent on the relative orientation of the symmetry axis with respect to the magnetic field, the energy spectra and thus the electromagnetic response of the NV centers to the applied fields are different for the four possible orientations.

*Selection Rules of Optical Transitions.*—According to Refs. [10, 12], there are four outer electrons distributed in the  $a_1$ ,  $e_x$  and  $e_y$  levels, i.e.  $a_1^2 e^2$ . On account of the spin degree of freedom, the electronic ground states are the triplet states labeled as [55]  $|\Phi_{A_2;1,0}^c\rangle$ ,  $|\Phi_{A_2;1,1}^c\rangle$ ,  $|\Phi_{A_2;1,-1}^c\rangle$ , where the superscript  $c$  means configuration, the subscripts are ordered as  $j, k; S, m_s$  with  $j$  being irreducible representation,  $k$  being row of irreducible representation,  $S$  being total spin and  $m_s$  being spin projection along the symmetry axis of the NV center. The six first-excited states, i.e.  $a_1 e^3$ , are [55]  $|\Phi_{E,x;1,0}^c\rangle$ ,  $|\Phi_{E,y;1,0}^c\rangle$ ,  $|\Phi_{E,x;1,1}^c\rangle$ ,  $|\Phi_{E,y;1,1}^c\rangle$ ,  $|\Phi_{E,x;1,-1}^c\rangle$ ,  $|\Phi_{E,y;1,-1}^c\rangle$ , where  $|\Phi_{E,x;S,m_s}^c\rangle$  and  $|\Phi_{E,y;S,m_s}^c\rangle$  are degenerate under a magnetic field. By comparing the ground and excited states, there is one electron transiting from the  $a_1$  orbital to the  $e$  orbital. Without spin-orbit coupling, due to conservation of spin and total angular momentum [11], the non-zero transition matrix elements of the position vector  $\vec{r} = x\hat{e}_x + y\hat{e}_y + z\hat{e}_z$  are in the following transitions  $|\Phi_{A_2;S,m_s}^c\rangle \xrightarrow{\alpha'} |\Phi_{E,\alpha;S,m_s}^c\rangle$  [12, 55], where  $\alpha, \alpha' = x, y$  and  $\alpha \neq \alpha'$ .

For the ground states, they can be formally diagonalized as  $|g_i\rangle = \sum_{j=-1}^1 C_{i,j}^g |\Phi_{A_2;1,j}^c\rangle$  ( $i = 1, 2, 3$ ) with eigenenergies  $E_i^g$ . And for the excited states, they can be formally diagonalized in two subsets according to their polarizations as  $|e_i^x\rangle = \sum_{j=-1}^1 C_{i,j}^e |\Phi_{E,x;1,j}^c\rangle$  and  $|e_i^y\rangle = \sum_{j=-1}^1 C_{i,j}^e |\Phi_{E,y;1,j}^c\rangle$  ( $i = 1, 2, 3$ ) with degenerate eigenenergies  $E_i^e$ , where they share the same coefficients due to the degeneracy.

According to Refs. [4, 13], the constitutive relation reads  $\vec{D} = \epsilon_0 \overleftrightarrow{\epsilon}_r \vec{E} = \epsilon_D \epsilon_0 \vec{E} + \vec{P}$ , where  $\vec{D}$  is the electric displacement,  $\epsilon_0$  is the electric permittivity of vacuum,  $\overleftrightarrow{\epsilon}_r$  and  $\epsilon_D$  are, respectively, the relative permittivity tensor of diamond with and without NV centers. The polarization density can be calculated using linear response theory [2, 9]

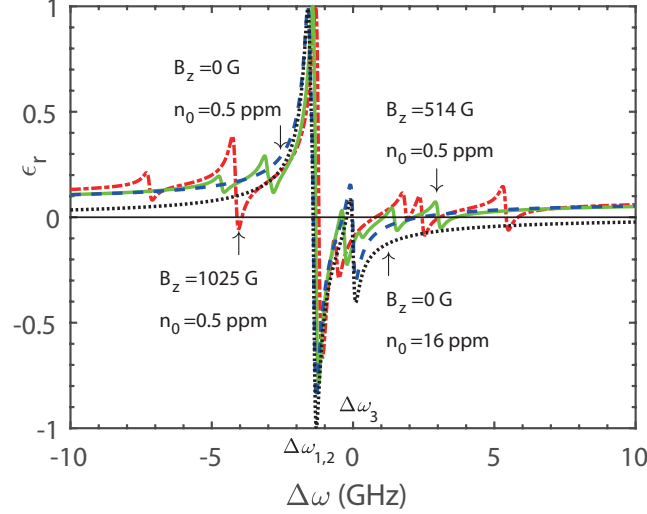


Figure 2. (color online) The frequency dependence of the electric permittivity  $\overleftrightarrow{\epsilon}_r$  of diamond with NV centers for different values of the magnetic field  $B$  and density of NV centers  $n_0$ : blue dashed line for  $B_z = 0$  G and  $n_0 = 0.5$  ppm, green solid line for  $B_z = 514$  G and  $n_0 = 0.5$  ppm, red dash-dotted line for  $B_z = 1025$  G and  $n_0 = 0.5$  ppm, black dotted line for  $B_z = 0$  G and  $n_0 = 16$  ppm. Other parameters are  $d_x = d_y = 11$  D [16],  $\gamma^{-1} = 10$  ns [17],  $\epsilon_D = 5.7$  [5], and  $\mu_D = 1 - 2.1 \times 10^{-5}$  [18],  $B_x = B_y = 0$  G. The thin black line  $\epsilon_r = 0$  is just a guide to the eye.

as

$$\vec{P} = -\frac{n_0}{\hbar} \text{Re} \sum_{j,i,f} \rho_i \frac{\vec{d}_{if}^{(j)} (\vec{d}_{fi}^{(j)} \cdot \vec{E})}{\omega - \Delta_{fi}^{(j)} + i\gamma}, \quad (3)$$

where  $\hbar$  is the Planck constant,  $n_0 = v_0^{-1}$  is the density of the NV centers,  $\rho_i$  is the probability of the initial state  $i$ ,  $\omega$  is the frequency of the electric field  $\vec{E}$ ,  $\Delta_{fi}^{(j)}$  is the transition frequency of the  $j$ th NV center between the initial state  $i$  and the final state  $f$ ,  $\gamma^{-1}$  is the lifetime of the final state  $f$ , and  $\vec{d}_{if}^{(j)}$  is the transition matrix element of the electric dipole of the  $j$ th NV center between the initial and final states. Note that  $i \neq f$  in Eq. (3), and also in Eq. (S83). In the above equation, we did not explicitly discriminate the contributions from  $|e_i^x\rangle$  and  $|e_i^y\rangle$ , as they only differ by the polarization direction.

The relative permittivity tensor is [55]

$$\overleftrightarrow{\epsilon}_r = \epsilon_D - \text{Re} \sum_{j,i,f,j_1,j_2} \frac{C_{i,j_1}^{g*}(j) C_{f,j_1}^e(j) C_{f,j_2}^{e*}(j) C_{i,j_2}^g(j)}{3\hbar\epsilon_0 v_0 \left\{ \omega - [E_f^e(j) - E_i^g(j)] + i\gamma \right\}} \times (\vec{d}_x^{(j)} + \vec{d}_y^{(j)}) (\vec{d}_x^{(j)} + \vec{d}_y^{(j)}), \quad (4)$$

where  $\vec{d}_x^{(j)}$  and  $\vec{d}_y^{(j)}$  are the components of the transition dipole of the  $j$ th NV center. Clearly, there can be nine possible negative permittivity components around the nine transition frequencies  $\Delta_{fi}^{(j)} = E_i^e(j) - E_f^g(j)$  of the  $j$ th NV center. However, if a static magnetic field is applied along the  $z$ -axis, all transition frequencies would be correspondingly identical for all four possible orientations [14]. Moreover, the relative permeability is not modified by the presence of NV centers because the transition  ${}^3A_2 \rightleftharpoons {}^3E$  can only be induced by the electric-dipole couplings to the electromagnetic field.

In Fig. 2 we investigate the dependence of the permittivity on the magnetic field and density of the NV centers. Noticeably, two of the three components of the permittivity remain unchanged and only one component is subtly modified by  $\vec{B}$  due to the symmetry and the special choice of  $\vec{B} \parallel \vec{e}_z$  [55]. As a special case, we plot the modified component of the permittivity  $\epsilon_r$  versus the frequency of the incident light for  $B = 0$ . When the magnetic field is absent, in the manifold of the electronic ground state,  $|\Phi_{A_2;1,\pm 1}^c\rangle$  are degenerate and there is an energy gap  $D_{\text{gs}}$  between them and  $|\Phi_{A_2;1,0}^c\rangle$ . For the manifold of the electronic excited state, because  $|\Phi_{E,\alpha;1,\pm 1}^c\rangle$  are degenerate, there would be level anti-crossing due to the strain-related coupling  $\xi$ . Since the electric-dipole induced transitions conserve the spin momentum [11], there could exist negative permittivity around three transition frequencies, i.e.

$\Delta\omega_{1,2} = D_{\text{es}}^{\parallel} - D_{\text{gs}} \pm \xi$  and  $\Delta\omega_3 = 0$  GHz [55]. However, in the blue dashed curve of Fig. 2, we can only observe two negative dips around the transition frequencies  $D_{\text{es}}^{\parallel} - D_{\text{gs}} = -1.46$  GHz and 0 GHz. The first two dips merge into a single one as their widths,  $\sim$  GHz, are much larger than their separation, i.e.  $2\xi = 0.14$  GHz. As the frequency of the incident light grows, the modified component of the permittivity eventually increases to become positive at  $\Delta\omega = 2.37$  GHz. Therefore, for  $B = 0$  and  $n_0 = 0.5$  ppm, the frequency window for demonstrating negative refraction is roughly  $(-1.46, 2.37)$  GHz. Because Eq. (S83) suggests negative permittivity to be around the transition frequencies, we hereafter explore the possibility of the negative refraction beyond the above frequency domain by tuning magnetic field. In the green solid curve of Fig. 2, we plot the permittivity at the degenerate point of the excited states, i.e.,  $B = 514$  G. A new negative dip appears at  $\Delta\omega = 3.11$  GHz. Interestingly, for the degenerate point of the ground states, i.e.,  $B = 1025$  G, in addition to the other two at  $\Delta\omega = 2.53$  GHz and  $\Delta\omega = 5.51$  GHz on the right, there is a new negative dip at  $\Delta\omega = -4.06$  GHz on the left hand side of  $\Delta\omega_{1,2}$ , cf. red dash-dotted curve of Fig. 2. Meanwhile, the depth of the main dip at  $\Delta\omega_{1,2}$  has been reduced as compared to the case when  $B = 0$  G. The increasing magnetic field does not only modify the transition frequencies, but also redistributes electric dipoles among the eigenstates. In this regard, by tuning the magnetic field, we can switch on/off the negative refraction on demand. In Fig. 2, there are only seven dips for the cases with  $B = 514$  G and  $B = 1025$  G, because there are two sets of degenerate eigenstates as shown in [55]. Furthermore, suggested by Eq. (S83), the permittivity is also influenced by the density  $n_0$  of the NV centers. In the black dotted curve of Fig. 2, this density is increased from  $n_0 = 0.5$  ppm to  $n_0 = 16$  ppm. Compared to the blue dashed curve of Fig. 2, the window of the negative refraction has been significantly broadened because more NV centers can negatively respond to the applied magnetic field. With this increased density, the negative dip at  $\Delta\omega = -4.06$  GHz can be more profound for  $B = 1025$  G. Notice that in the numerical simulation we have not used the local field correction [4, 13], since the local field correction will not substantially change the center and width of the negative refraction domain but will modify its magnitude [7–9, 55]. Therefore, we have demonstrated negative refraction by the normalized  $\epsilon_r$  in Fig. 2.

*Negative Refraction.*—In Ref. [1], it has been shown that for a double-negative metamaterial there can be negative refraction. However, in the NV centers of diamond, because the electric permittivity tensor possesses two different components, it is natural to ask whether negative refraction can exist. Below, we will demonstrate that negative refraction can indeed occur for a TH incident mode [55], cf. Fig. 1(b).

According to Maxwell's equations [4, 13],  $\nabla \times \vec{E} = -\frac{\partial}{\partial t} \mu_D \vec{H}$ ,  $\nabla \times \vec{H} = \frac{\partial}{\partial t} \overleftrightarrow{\epsilon} \vec{E}$ , where both the current density and the charge density vanish,  $\overleftrightarrow{\epsilon} = \epsilon_0 \overleftrightarrow{\epsilon}_r$  is the permittivity of diamond with NV centers, and  $\mu_D$  is the permeability of pure diamond.

Assuming that the transmitted electric and magnetic fields are, respectively,  $\vec{E}_t(\vec{r}, t) = (E_{tx}\hat{e}_x + E_{tz}\hat{e}_z) \exp[i(\vec{k}_t \cdot \vec{r} - \omega t)]$ ,  $\vec{H}_t(\vec{r}, t) = H_{ty}\hat{e}_y \exp[i(\vec{k}_t \cdot \vec{r} - \omega t)]$ , we have

$$(\nabla \times \nabla \times \overleftrightarrow{I} - \mu_0 \omega^2 \overleftrightarrow{\epsilon}) \vec{E}_t = 0, \quad (5)$$

where  $\overleftrightarrow{I}$  is the identity dyadic. For nontrivial solutions, the dispersion relation for the extraordinary mode reads

$$\epsilon_x k_{tx}^2 + \epsilon_z k_{tz}^2 = \mu_0 \omega^2 \epsilon_x \epsilon_z, \quad (6)$$

assuming  $k_y = 0$ . Such a dispersion relation for the extraordinary mode is hyperbolic or indefinite because  $\epsilon_x \epsilon_z < 0$ .

According to the boundary condition [4], the tangential components of the wavevector across the interface should be equal, i.e.,  $k_{tz} = k_{iz} > 0$ ,  $k_{tx} = k_{ix}$ . By inserting Eq. (S121) into Eq. (S116), we obtain the relation between  $E_{tx}$  and  $E_{tz}$  as  $\epsilon_x k_{tx} E_{tx} + \epsilon_z k_{tz} E_{tz} = 0$ . By Maxwell equation, we have

$$\vec{H} = -\frac{\omega \epsilon_z E_{tz}}{k_{tx}} \hat{e}_y \exp \left[ i \left( \vec{k}_t \cdot \vec{r} - \omega t \right) \right]. \quad (7)$$

The time-averaged Poynting vector reads [4]  $\vec{S}_t = \frac{1}{2} \text{Re}(\vec{E}_t \times \vec{H}_t^*)$ , with the components being  $S_{tx} = \frac{\omega \epsilon_z}{2k_{tx}} E_{tz}^2$ ,  $S_{tz} = \frac{\epsilon_x \omega E_{tx}^2}{2k_{tz}} < 0$ , because  $\epsilon_x < 0$  and  $\omega, k_{tz} > 0$ . In order to transmit energy from the interface into the medium,  $S_{tx}$  should be negative and thus  $k_{tx} < 0$  as  $\omega, \epsilon_z > 0$ . Together with Eq. (S121), we have

$$k_{tx} = -k_i \sqrt{\frac{\epsilon_z}{\epsilon_0} \left( 1 - \frac{\epsilon_0}{\epsilon_x} \sin^2 \theta \right)}, \quad (8)$$

where  $k_i^2 = \mu_0 \epsilon_0 \omega^2$ . Because  $S_{tx}, S_{tz} < 0$ , we have proven that for a uniaxial crystal with hyperbolic dispersion, the negative refraction exists for a TH incident field.

*Experimental Feasibility.*—For zero magnetic field, the Hamiltonians of the electronic ground and excited states are further simplified as  $H_{gs} = D_{gs} \sum_{m_z=\pm 1} |\Phi_{A_2;1,m_z}^c\rangle \langle \Phi_{A_2;1,m_z}^c|$  and  $H_{es} \simeq \sum_{\alpha=x,y} \sum_{m_z=\pm 1} D_{es}^{\parallel} |\Phi_{E,\alpha;1,m_z}^c\rangle \langle \Phi_{E,\alpha;1,m_z}^c|$  [55], where we have omitted the strain-related coupling.

The transition electric dipole has been estimated as 11 D [16]. For simplicity, the orientations of all NV centers are assumed to be along the  $z$ -axis. Thus, all matrix elements of the transition electric dipole are equal to  $\vec{d}_{if} = \langle \Phi_{A_2;1,m_z}^c | \vec{d} | \Phi_{E,\alpha;1,m_z}^c \rangle = 11(\hat{e}_x + \hat{e}_y) D$ . Initially, the NV center is in the thermal state  $\rho(0) = \frac{1}{3} \sum_{m_z=\pm 1} |\Phi_{A_2;S,m_s}^c\rangle \langle \Phi_{A_2;S,m_s}^c|$ . Therefore,  $\sum_{i,f} \vec{d}_{if} \vec{d}_{fi} = \frac{484}{3} (\hat{e}_x \hat{e}_x + \hat{e}_y \hat{e}_y + \hat{e}_x \hat{e}_y + \hat{e}_y \hat{e}_x) D^2$ , and

$$\vec{P} = -2\zeta\gamma\epsilon_0 \text{Re} \left[ \frac{(\hat{e}_x \hat{e}_x + \hat{e}_y \hat{e}_y + \hat{e}_x \hat{e}_y + \hat{e}_y \hat{e}_x) \vec{E}}{\omega - \Delta_{fi} + i\gamma} \right], \quad (9)$$

where  $\zeta = \frac{242n_0 D^2}{9\hbar\gamma\epsilon_0}$ . The three principal components of the relative permittivity are, respectively,

$$\epsilon_r^{(1)} = \epsilon_D - \frac{2\zeta\gamma(\omega - \Delta_{fi})}{(\omega - \Delta_{fi})^2 + \gamma^2}, \quad (10)$$

$\epsilon_r^{(2)} = \epsilon_r^{(3)} = \epsilon_D$ . When the frequency of the incident field is  $\omega = \Delta_{fi} + \gamma$ , one principal component can be negative if  $n_0 > n_0^c = 1.77 \times 10^{21} \text{ m}^{-3}$ , while the other principal components remain positive. Because two carbon atoms occupy a volume  $v = (1.78 \times 10^{-10})^3 \text{ m}^{-3}$ , the minimum density of the NV centers to demonstrate negative refraction is

$$\frac{1}{2}vn_0^c = 5.00 \text{ ppb}, \quad (11)$$

which is feasible in experimental fabrication, e.g. 16 ppm [20]. In addition, as proven in [55], the negative component of permittivity appears in the  $z$ -axis, because of  $\vec{B} \parallel \vec{e}_z$  and the symmetry of four possible orientations of the NV centers.

*Conclusions.*—In this work, we proposed a new approach to realize hyperbolic metamaterial using diamond with NV centers in the optical frequency regime. Because of the long lifetime of the excited states of the NV centers, this hyperbolic metamaterial manifests an intriguing window for negative refraction. By varying the applied magnetic field to tune the energy spectra of both ground and excited states, the frequency of the negative refraction can be tuned in a wide range. Note that it is difficult to fabricate classical metamaterials working in optical-frequency domain, because the sizes of the elements therein are sub-micron. The NV-metamaterials proposed here solve this problem. Because this NV-metamaterial can be used in subwavelength imaging, spontaneous emission enhancement, heat transport and acoustics, analogue cosmology, and lifetime engineering, our proposal bridges the gap between NV centers and metamaterials.

We thank stimulating discussion with Zhou Li and K. Y. Bliokh. This work was supported by the MURI Center for Dynamic Magneto-Optics via the AFOSR Award No. FA9550-14-1-0040, the Japan Society for the Promotion of Science (KAKENHI), the IMPACT program of JST, JSPS-RFBR grant No. 17-52-50023, CREST grant No. JPMJCR1676, and RIKEN-AIST Challenge Research Fund. C.P.S. was supported by NSFC under Grant No. 11421063 and No. 11534002, NSAF under Grant No. U1530401. Q.A. was partially supported by NSFC under Grant No. 11505007.

- 
- [1] V. G. Veselago, The electrodynamics of substances with simultaneously negative values of  $\epsilon$  and  $\mu$ , *Sov. Phys. Uspekhi.* **10**, 509 (1968).
  - [2] J. B. Pendry, Negative refraction makes a perfect lens, *Phys. Rev. Lett.* **85**, 3966 (2000).
  - [3] D. R. Smith, W. J. Padilla, D. C. Vier, S. C. Nemat-Nasser, and S. Schultz, Composite medium with simultaneously negative permeability and permittivity, *Phys. Rev. Lett.* **84**, 4184 (2000).
  - [4] K. Y. Bliokh, Y. P. Bliokh, V. Freilikher, S. Savel'ev, and F. Nori, Colloquium: Unusual resonators: Plasmonics, metamaterials, and random media, *Rev. Mod. Phys.* **80**, 1201 (2008).
  - [5] Y. Shen and Q. Ai, Optical properties of drug metabolites in latent fingerprints, *Sci. Rep.* **6**, 20336 (2016).
  - [6] Y. P. Bliokh, V. Freilikher, and F. Nori, Ballistic charge transport in graphene and light propagation in periodic dielectric structures with metamaterials: A comparative study, *Phys. Rev. B* **87**, 245134 (2013).
  - [7] A. V. Kats, S. Savel'ev, V. A. Yampol'skii, and F. Nori, Left-handed interfaces for electromagnetic surface waves, *Phys. Rev. Lett.* **98**, 073901 (2007).
  - [8] J. Yao, Z. Liu, Y. Liu, Y. Wang, C. Sun, G. Bartal, A. M. Stacy, and X. Zhang, Optical negative refraction in bulk metamaterials of nanowires, *Science* **321**, 930 (2008).

- [9] Y. N. Fang, Y. Shen, Q. Ai, and C. P. Sun, Negative refraction in Möbius molecules, *Phys. Rev. A* **94**, 043805 (2016).
- [10] C. W. Chang, M. Liu, S. Nam, S. Zhang, Y. Liu, G. Bartal, and X. Zhang, Optical Möbius symmetry in metamaterials, *Phys. Rev. Lett.* **105**, 235501 (2010).
- [11] Y. Shen, H. Y. Ko, Q. Ai, S. M. Peng, and B. Y. Jin, Molecular split-ring resonators based on metal string complexes, *J. Phys. Chem. C* **118**, 3766 (2014).
- [12] A. L. Rakhmanov, V. A. Yampol'skii, J. A. Fan, F. Capasso, and F. Nori, Layered superconductors as negative-refractive-index metamaterials, *Phys. Rev. B* **81**, 075101 (2010).
- [13] A. Poddubny, I. Iorsh, P. Belov, and Y. Kivshar, Hyperbolic metamaterials, *Nat. Photon.* **7**, 958 (2013).
- [14] S. Jahani and Z. Jacob, All-dielectric metamaterials, *Nat. Nanotechnol.* **11**, 23 (2016).
- [15] D. R. Smith and D. Schurig, Electromagnetic wave propagation in media with indefinite permittivity and permeability tensors, *Phys. Rev. Lett.* **90**, 077405 (2003).
- [16] P. A. Belov, Backward waves and negative refraction in uniaxial dielectrics with negative dielectric permittivity along the anisotropy axis, *Microw. Opt. Technol. Lett.* **37**, 259 (2003).
- [17] Z. Liu, H. Lee, Y. Xiong, C. Sun, and X. Zhang, Far-field optical hyperlens magnifying sub-diffraction-limited objects, *Science* **315**, 1686 (2007).
- [18] S. Ishii, A. V. Kildishev, E. Narimanov, V. M. Shalaev, and V. P. Drachev, Sub-wavelength interference pattern from volume plasmon polaritons in a hyperbolic medium, *Las. Photon. Rev.* **7**, 265 (2013).
- [19] Z. Jacob, I. Smolyaninov, and E. Narimanov, Broadband Purcell effect: radiative decay engineering with metamaterials, *Appl. Phys. Lett.* **100**, 181105 (2012).
- [20] S. A. Biehs, M. Tschikin, and P. Ben-Abdallah, Hyperbolic metamaterials as an analog of a blackbody in the near field, *Phys. Rev. Lett.* **109**, 104301 (2012).
- [21] J. Li, L. Fok, X. Yin, G. Bartal, and X. Zhang, Experimental demonstration of an acoustic magnifying hyperlens, *Nature Mater.* **8**, 931 (2009).
- [22] I. I. Smolyaninov and E. E. Narimanov, Metric signature transitions in optical metamaterials, *Phys. Rev. Lett.* **105**, 067402 (2010).
- [23] H. N. S. Krishnamoorthy, Z. Jacob, E. Narimanov, I. Kretzschmar, and V. M. Menon, Topological transitions in metamaterials, *Science* **336**, 205 (2012).
- [24] X. Yang, J. Yao, J. Rho, X. Yin, and X. Zhang, Experimental realization of three-dimensional indefinite cavities at the nanoscale with anomalous scaling laws, *Nature Photon.* **6**, 450 (2012).
- [25] R. Schirhagl, K. Chang, M. Loretz, and C. L. Degen, Nitrogen-vacancy centers in diamond: Nanoscale sensors for physics and biology, *Annu. Rev. Phys. Chem.* **65**, 83 (2014).
- [26] Y. Wu, F. Jelezko, M. B. Plenio, and T. Weil, Diamond Quantum Devices in Biology, *Angew. Chem., Int. Ed.* **55**, 6586 (2016).
- [27] M. W. Doherty, N. B. Manson, P. Delaney, F. Jelezko, J. Wrachtrup, and L. C. L. Hollenberg, The nitrogen-vacancy colour centre in diamond, *Phys. Rep.* **528**, 1 (2013).
- [28] M. Chen, C. Meng, Q. Zhang, C. Duan, F. Shi, and J. F. Du, Quantum metrology with single spins in diamond under ambient conditions, *Natl. Sci. Rev.* in press (2017).
- [29] J. Jeske, D. W. M. Lau, X. Vidal, L. P. McGuinness, P. Reineck, B. C. Johnson, M. W. Doherty, J. C. McCallum, S. Onoda, F. Jelezko, T. Ohshima, T. Volz, J. H. Cole, B. C. Gibson, and A. D. Greentree, Stimulated emission from nitrogen-vacancy centres in diamond, *Nature Commun.* **8**, 14000 (2017).
- [30] L. Jin, M. Pfender, N. Aslam, P. Neumann, S. Yang, J. Wrachtrup, and R.-B. Liu, Proposal for a room-temperature diamond maser, *Nature Commun.* **6**, 8251 (2015).
- [31] M. P. Ledbetter, K. Jensen, R. Fischer, A. Jarmola, and D. Budker, Gyroscopes based on nitrogen-vacancy centers in diamond, *Phys. Rev. A* **86**, 052116 (2012).
- [32] B. B. Zhou, A. Baksic, H. Ribeiro, C. G. Yale, F. J. Heremans, P. C. Jerger, A. Auer, G. Burkard, A. A. Clerk, and D. D. Awschalom, Accelerated quantum control using superadiabatic dynamics in a solid-state lambda system, *Nat. Phys.* **13**, 330 (2017).
- [33] X. K. Song, Q. Ai, J. Qiu, and F. G. Deng, Physically feasible three-level transitionless quantum driving with multiple Schrödinger dynamics, *Phys. Rev. A* **93**, 052324 (2016).
- [34] F. Dolde, H. Fedder, M. W. Doherty, T. Nobauer, F. Rempp, G. Balasubramanian, T. Wolf, F. Reinhard, L. C. L. Hollenberg, F. Jelezko, and J. Wrachtrup, Electric-field sensing using single diamond spins, *Nat. Phys.* **7**, 459 (2011).
- [35] F. Dolde, M. W. Doherty, J. Michl, I. Jakobi, B. Naydenov, S. Pezzagna, J. Meijer, P. Neumann, F. Jelezko, N. B. Manson, and J. Wrachtrup, Nanoscale Detection of a Single Fundamental Charge in Ambient Conditions Using the NV<sup>-</sup> Center in Diamond, *Phys. Rev. Lett.* **112**, 097603 (2014).
- [36] J. R. Maze, P. L. Stanwix, J. S. Hodges, S. Hong, J. M. Taylor, P. Cappellaro, L. Jiang, M. V. G. Dutt, E. Togan, A. S. Zibrov, A. Yacoby, R. L. Walsworth, and M. D. Lukin, Nanoscale magnetic sensing with an individual electronic spin in diamond, *Nature (London)* **455**, 644 (2008).
- [37] G. Balasubramanian, I. Y. Chan, R. Kolesov, M. Al-Hmoud, J. Tisler, C. Shin, C. Kim, A. Wojcik, P. R. Hemmer, A. Krueger, T. Hanke, A. Leitenstorfer, R. Bratschitsch, F. Jelezko, and J. Wrachtrup, Nanoscale imaging magnetometry with diamond spins under ambient conditions, *Nature (London)* **455**, 648 (2008).
- [38] L. S. Li, H. H. Li, L. L. Zhou, Z. S. Yang, and Q. Ai, Measurement of weak static magnetic fields with nitrogen-vacancy color center, *Acta. Phys. Sin.* **66**, 230601 (2017).
- [39] N. Zhao, J.-L. Hu, S.-W. Ho, T.-K. Wen, and R. B. Liu, Atomic-scale magnetometry of distant nuclear spin clusters via nitrogen-vacancy spin in diamond, *Nat. Nanotechnol.* **6**, 242 (2011).

- [40] M. S. Grinolds, S. Hong, P. Maletinsky, L. Luan, M. D. Lukin, R. L. Walsworth, and A. Yacoby, Nanoscale magnetic imaging of a single electron spin under ambient conditions, *Nat. Phys.* **9**, 215 (2013).
- [41] A. Cooper, E. Magesan, H. Yum, and P. Cappellaro, Time-resolved magnetic sensing with electronic spins in diamond, *Nat. Commun.* **5**, 3141 (2014).
- [42] F. Shi, Q. Zhang, P. Wang, H. Sun, J. Wang, X. Rong, M. Chen, C. Ju, F. Reinhard, H. Chen, J. Wrachtrup, J. Wang, and J. F. Du, Single-protein spin resonance spectroscopy under ambient conditions, *Science* **347**, 1135 (2015).
- [43] S. J. DeVience, L. M. Pham, I. Lovchinsky, A. O. Sushkov, N. Bar-Gill, C. Belthangady, F. Casola, M. Corbett, H. Zhang, M. Lukin, H. Park, A. Yacoby, and R. L. Walsworth, Nanoscale NMR spectroscopy and imaging of multiple nuclear species, *Nat. Nanotechnol.* **10**, 129 (2015).
- [44] J. M. Boss, K. Chang, J. Armijo, K. Cujia, T. Rosskopf, J. R. Maze, and C. L. Degen, One- and two-dimensional nuclear magnetic resonance spectroscopy with a diamond quantum sensor, *Phys. Rev. Lett.* **116**, 197601 (2016).
- [45] H. B. Liu, M. B. Plenio, and J.-M. Cai, Scheme for detection of single-molecule radical pair reaction using spin in diamond, *Phys. Rev. Lett.* **118**, 200402 (2017).
- [46] Y.-Y. Wang, J. Qiu, Y.-Q. Chu, M. Zhang, J.-M. Cai, Q. Ai, and F.-G. Deng, Dark state polarizing a nuclear spin in the vicinity of a nitrogen-vacancy center, arXiv:1708.05467 (2017).
- [47] G. Kucsko, P. C. Maurer, N. Y. Yao, M. Kubo, H. J. Noh, P. K. Lo, H. Park, and M. D. Lukin, Nanometre-scale thermometry in a living cell, *Nature (London)* **500**, 54 (2013).
- [48] D. M. Toyli, C. F. de las Casas, D. J. Christle, V. V. Dobrovitski, and D. D. Awschalom, Fluorescence thermometry enhanced by the quantum coherence of single spins in diamond, *Proc. Natl. Acad. Sci. U.S.A.* **110**, 8417 (2013).
- [49] P. Neumann, I. Jakobi, F. Dolde, C. Burk, R. Reuter, G. Waldherr, J. Honert, T. Wolf, A. Brunner, J. H. Shim, D. Suter, H. Sumiya, J. Isoya, and J. Wrachtrup, High-precision nanoscale temperature sensing using single defects in diamond, *Nano Lett.* **13**, 2738 (2013).
- [50] Z.-L. Xiang, S. Ashhab, J. Q. You, and F. Nori, Hybrid quantum circuits: Superconducting circuits interacting with other quantum systems, *Rev. Mod. Phys.* **85**, 623 (2013).
- [51] Z.-L. Xiang, X.-Y. Lü, T.-F. Li, J. Q. You, and F. Nori, Hybrid quantum circuit consisting of a superconducting flux qubit coupled to a spin ensemble and a transmission-line resonator, *Phys. Rev. B* **87**, 144516 (2013).
- [52] X.-Y. Lü, Z.-L. Xiang, W. Cui, J. Q. You, and F. Nori, Quantum memory using a hybrid circuit with flux qubits and nitrogen-vacancy centers, *Phys. Rev. A* **88**, 012329 (2013).
- [53] P.-B. Li, Z.-L. Xiang, P. Rabl, and F. Nori, Hybrid quantum device with nitrogen-vacancy centers in diamond coupled to carbon nanotubes, *Phys. Rev. Lett.* **117**, 015502 (2016).
- [54] A. M. Zagoskin, J. R. Johansson, S. Ashhab, and F. Nori, Quantum information processing using frequency control of impurity spins in diamond, *Phys. Rev. B* **76**, 014122 (2007).
- [55] See Supplemental material for details of calculation, which includes Refs. [1, 2, 4, 5, 7–20].
- [56] L. J. Zou, D. Marcos, S. Diehl, S. Putz, J. Schmiedmayer, J. Majer, and P. Rabl, Implementation of the Dicke lattice model in hybrid quantum system arrays, *Phys. Rev. Lett.* **113**, 023603 (2014).
- [57] J. J. Sakurai, *Modern Quantum Mechanics* (Addison-Wesley, Reading, MA, 1993).
- [58] M. W. Doherty, N. B. Manson, P. Delaney, and L. C. L. Hollenberg, The negatively charged nitrogen-vacancy centre in diamond: the electronic solution, *New J. Phys.* **13**, 025019 (2011).
- [59] J. R. Maze, A. Gali, E. Togan, Y. Chu, A. Trifonov, E. Kaxiras, and M. D. Lukin, Properties of nitrogen-vacancy centers in diamond: the group theoretic approach, *New J. Phys.* **13**, 025025 (2011).
- [60] E. Togan, Y. Chu, A. S. Trifonov, L. Jiang, J. Maze, L. Childress, M. V. G. Dutt, A. S. Sørensen, P. R. Hemmer, A. S. Zibrov, and M. D. Lukin, Quantum entanglement between an optical photon and a solid-state spin qubit, *Nature (London)* **466**, 730 (2010).
- [61] J. D. Jackson, *Classical Electrodynamics* 3rd ed., (John Wiley, United States, 1999).
- [62] L. D. Landau, E. M. Lifshitz, and L. P. Pitaevskii, *Electrodynamics of Continuous Media* 2nd Ed., (Butterworth Heinmann, Oxford, 1995).
- [63] R. Kubo, M. Toda, and N. Hashitsume, *Statistical Physics II Nonequilibrium Statistical Mechanics* (Springer-Verlag, Berlin Heidelberg, 1985).
- [64] J. Kästel, M. Fleischhauer, S. F. Yelin, and R. L. Walsworth, Tunable negative refraction without absorption via electromagnetically induced chirality, *Phys. Rev. Lett.* **99**, 073602 (2007).
- [65] J. Kästel, M. Fleischhauer, and G. Juzeliūnas, Local-field effects in magnetodielectric media: Negative refraction and absorption reduction, *Phys. Rev. A* **76**, 062509 (2007).
- [66] A. Lenef, S. W. Brown, D. A. Redman, and S. C. Rand, Electronic structure of the N-V center in diamond: Experiments, *Phys. Rev. B* **53**, 13427 (1996).
- [67] V. M. Acosta, Optical magnetometry with nitrogen-vacancy centers in diamond, Ph.D. thesis, University of California, Berkeley, 2011.
- [68] J. Fontanella, R. L. Johnston, J. H. Colwell, and C. Andeen, Temperature and pressure variation of the refractive index of diamond, *Appl. Opt.* **16**, 2949 (1977).
- [69] H. D. Young, *University Physics* 7th Ed., (Addison Wesley, San Francisco, 1992).
- [70] A. Jarmola, V. M. Acosta, K. Jensen, S. Chemerisov, and D. Budker, Temperature- and magnetic-field-dependent longitudinal spin relaxation in nitrogen-vacancy ensembles in diamond, *Phys. Rev. Lett.* **108**, 197601 (2012).

## SI. MODEL

The Hamiltonian of an NV center in its electronic *ground* state is [S1]

$$\begin{aligned}
H_{\text{gs}} = & D_{\text{gs}} \left[ S_z^2 - \frac{1}{3} S(S+1) \right] + A_{\text{gs}}^{\parallel} S_z I_z + A_{\text{gs}}^{\perp} (S_x I_x + S_y I_y) + P_{\text{gs}} \left[ I_z^2 - \frac{1}{3} I(I+1) \right] \\
& + \mu_B g_{\text{gs}}^{\parallel} B_z S_z + \mu_B g_{\text{gs}}^{\perp} (B_x S_x + B_y S_y) + \mu_N g_N \vec{B} \cdot \vec{I} \\
& + d_{\text{gs}}^{\parallel} (E_z + \delta_z) \left[ S_z^2 - \frac{1}{3} S(S+1) \right] + d_{\text{gs}}^{\perp} (E_x + \delta_x) (S_y^2 - S_x^2) + d_{\text{gs}}^{\perp} (E_y + \delta_y) (S_x S_y + S_y S_x). \quad (\text{S1})
\end{aligned}$$

Here,  $D_{\text{gs}} = 2.88$  GHz is the zero-field splitting of the electronic ground state;  $A_{\text{gs}}^{\parallel}$  and  $A_{\text{gs}}^{\perp}$  are the axial and non-axial components of hyperfine interaction tensor of the electronic ground state;  $I_x$ ,  $I_y$ ,  $I_z$  are the spin operators of the nuclear spin;  $P_{\text{gs}}$  is the nuclear electric quadruple parameter of the electronic ground state;  $\mu_B$  and  $\mu_N$  are the Bohr magneton and nuclear magneton respectively;  $g_{\text{gs}}^{\parallel} \simeq g_{\text{gs}}^{\perp} = g_{\text{gs}} \simeq 2$  and  $g_N$  are respectively the  $g$ -factors of electronic ground state and nuclear spin;  $d_{\text{gs}}^{\parallel} = 3.377 \times 10^{-5}$  D and  $d_{\text{gs}}^{\perp} = 6.9525 \times 10^{-7}$  D are the components of electric dipole moment of the electronic ground state;  $\vec{E}$ ,  $\vec{B}$ , and  $\vec{\delta}$  are the electric, magnetic and strain fields respectively. The electron spin operators in the basis  $\{|+\rangle, |0\rangle, |-\rangle\}$  are

$$S_x = \frac{1}{\sqrt{2}} \begin{pmatrix} 0 & 1 & 0 \\ 1 & 0 & 1 \\ 0 & 1 & 0 \end{pmatrix}, \quad (\text{S2})$$

$$S_y = \frac{i}{\sqrt{2}} \begin{pmatrix} 0 & -1 & 0 \\ 1 & 0 & -1 \\ 0 & 1 & 0 \end{pmatrix}, \quad (\text{S3})$$

$$S_z = \begin{pmatrix} 1 & 0 & 0 \\ 0 & 0 & 0 \\ 0 & 0 & -1 \end{pmatrix}. \quad (\text{S4})$$

When there is no nuclear spin, electric and strain fields, the Hamiltonian of the electronic ground state is simplified as

$$\begin{aligned}
H_{\text{gs}} = & D_{\text{gs}} S_z^2 + \mu_B g_{\text{gs}}^{\parallel} B_z S_z + \mu_B g_{\text{gs}}^{\perp} (B_x S_x + B_y S_y) \\
= & \begin{pmatrix} D_{\text{gs}} + \mu_B g_{\text{gs}}^{\parallel} B_z & \frac{1}{\sqrt{2}} \mu_B g_{\text{gs}}^{\perp} (B_x - i B_y) & 0 \\ \frac{1}{\sqrt{2}} \mu_B g_{\text{gs}}^{\perp} (B_x + i B_y) & 0 & \frac{1}{\sqrt{2}} \mu_B g_{\text{gs}}^{\perp} (B_x - i B_y) \\ 0 & \frac{1}{\sqrt{2}} \mu_B g_{\text{gs}}^{\perp} (B_x + i B_y) & D_{\text{gs}} - \mu_B g_{\text{gs}}^{\parallel} B_z \end{pmatrix}. \quad (\text{S5})
\end{aligned}$$

At room temperature, the Hamiltonian of an NV center in the electronic *excited* state is [S1]

$$\begin{aligned}
H_{\text{es}} = & D_{\text{es}}^{\parallel} \left[ S_z^2 - \frac{1}{3} S(S+1) \right] + A_{\text{es}}^{\parallel} S_z I_z + A_{\text{es}}^{\perp} (S_x I_x + S_y I_y) + P_{\text{es}} \left[ I_z^2 - \frac{1}{3} I(I+1) \right] \\
& + \mu_B g_{\text{es}}^{\text{RT}} \vec{B} \cdot \vec{S} + d_{\text{es}}^{\parallel} (E_z + \delta_z) \left[ S_z^2 - \frac{1}{3} S(S+1) \right] + \xi (S_y^2 - S_x^2), \quad (\text{S6})
\end{aligned}$$

where  $D_{\text{es}}^{\parallel} = 1.42$  GHz is the zero-field splitting of the electronic excited state;  $A_{\text{es}}^{\parallel}$  and  $A_{\text{es}}^{\perp}$  are the axial and non-axial components of hyperfine interaction tensor of the electronic excited state;  $P_{\text{es}}$  is the nuclear electric quadruple parameter of the electronic excited state;  $g_{\text{es}}^{\text{RT}} \simeq 2.01$  is the  $g$ -factor of electronic spin of excited state at the room temperature;  $d_{\text{es}}^{\parallel} = 1.192$  D is the electric dipole moment of the excited state;  $\xi = 70$  MHz is the strain-related coupling. When there is no nuclear spin, electric and strain fields, the Hamiltonian of the electronic excited state is simplified as

$$\begin{aligned}
H_{\text{es}} = & D_{\text{es}}^{\parallel} S_z^2 + \mu_B g_{\text{es}}^{\text{RT}} \vec{B} \cdot \vec{S} + \xi (S_y^2 - S_x^2) \\
= & \begin{pmatrix} D_{\text{es}}^{\parallel} + \mu_B g_{\text{es}}^{\text{RT}} B_z & \frac{1}{\sqrt{2}} \mu_B g_{\text{es}}^{\text{RT}} (B_x - i B_y) & -\xi \\ \frac{1}{\sqrt{2}} \mu_B g_{\text{es}}^{\text{RT}} (B_x + i B_y) & 0 & \frac{1}{\sqrt{2}} \mu_B g_{\text{es}}^{\text{RT}} (B_x - i B_y) \\ -\xi & \frac{1}{\sqrt{2}} \mu_B g_{\text{es}}^{\text{RT}} (B_x + i B_y) & D_{\text{es}}^{\parallel} - \mu_B g_{\text{es}}^{\text{RT}} B_z \end{pmatrix}. \quad (\text{S7})
\end{aligned}$$



## SII. LINEAR RESPONSE THEORY

In order to simulate the electromagnetic response of the diamond with NV centers in the presence of applied fields, we can employ the linear-response theory [S2] to calculate the electric permittivity and magnetic permeability. When there is an electric field applied, the NV center is polarized as

$$\langle \vec{d} \rangle = \int \frac{d\omega}{2\pi} S(\omega) \vec{E}(\omega) e^{-i\omega t}, \quad (\text{S8})$$

where the Fourier transform of the time-dependent electric field with amplitude  $\vec{E}_0$  and frequency  $\omega$

$$\vec{E}(t) = \vec{E}_0 \cos \omega t \quad (\text{S9})$$

is

$$\vec{E}(\omega) = \int_{-\infty}^{\infty} dt \vec{E}(t) e^{i\omega t}, \quad (\text{S10})$$

$$S(\omega) = -J(\omega) - J^*(-\omega). \quad (\text{S11})$$

Here,  $J(\omega)$  is the dipole-dipole correlation function,

$$J(\omega) = -i \int_0^{\infty} dt \text{Tr}[\vec{d}(t) \vec{d} \rho_0] e^{i\omega t}, \quad (\text{S12})$$

where the initial state of the NV center is

$$\rho_0 = \sum_i \rho_i |k_i\rangle \langle k_i| \quad (\text{S13})$$

with  $\sum_i \rho_i = 1$ .

The electric dipole in the Heisenberg picture is

$$\vec{d}(t) = \exp(iH^\dagger t/\hbar) \vec{d} \exp(-iHt/\hbar), \quad (\text{S14})$$

where

$$H = H_{\text{es}} \otimes |e\rangle \langle e| + H_{\text{gs}} \otimes |g\rangle \langle g|, \quad (\text{S15})$$

with  $|g\rangle$  ( $|e\rangle$ ) being the electronic ground (excited) state. Because the Fourier transform of the electric field is

$$\vec{E}(\omega_1) = \int_{-\infty}^{\infty} dt \vec{E}_0 \cos \omega t e^{i\omega_1 t} = \pi \vec{E}_0 [\delta(\omega_1 + \omega) + \delta(\omega_1 - \omega)], \quad (\text{S16})$$

the electric dipole of the NV center in the applied electric field is

$$\langle \vec{d} \rangle = \int \frac{d\omega_1}{2\pi} S(\omega_1) e^{-i\omega_1 t} \pi \vec{E}_0 [\delta(\omega_1 + \omega) + \delta(\omega_1 - \omega)] = -\vec{E}_0 \text{Re}\{[J(\omega) + J^*(-\omega)] e^{-i\omega t}\}, \quad (\text{S17})$$

where

$$\begin{aligned} J(\omega) &= -i \int_0^{\infty} dt e^{i\omega t} \sum_i \rho_i \langle k_i | \vec{d}(t) \vec{d} | k_i \rangle \\ &= -i \int_0^{\infty} dt e^{i\omega t} \sum_i \rho_i \langle k_i | e^{iH^\dagger t/\hbar} \vec{d} e^{-iHt/\hbar} \vec{d} | k_i \rangle \\ &= -i \int_0^{\infty} dt e^{i\omega t} \sum_{i, k_1, k_2, k_3} \rho_i \langle k_i | e^{iH^\dagger t/\hbar} | k_1 \rangle \langle k_1 | \vec{d} | k_2 \rangle \langle k_2 | e^{-iHt/\hbar} | k_3 \rangle \langle k_3 | \vec{d} | k_i \rangle \\ &= -i \int_0^{\infty} dt e^{i\omega t} \sum_{i, f} \rho_i e^{i(H_{k_i}^\dagger - H_{k_f})t/\hbar} \vec{d}_{k_i, k_f} \vec{d}_{k_f, k_i} \\ &= -i \int_0^{\infty} dt \sum_{i, f} \rho_i e^{i(\omega - \Delta_{k_f k_i} + i\gamma)t} \vec{d}_{k_i, k_f} \vec{d}_{k_f, k_i} \\ &= \sum_{i, f} \rho_i \frac{\vec{d}_{k_i, k_f} \vec{d}_{k_f, k_i}}{\omega - \Delta_{k_f k_i} + i\gamma}, \end{aligned} \quad (\text{S18})$$

where in the sum the final state should be different from the initial state, i.e.,  $i \neq f$ ,

$$H_{k_i} = \langle k_i | H | k_i \rangle = E_{k_i} - \frac{i}{2}\gamma \quad (\text{S19})$$

with  $-i\gamma/2$  being phenomenologically introduced for the decay of the excited state. Here,  $\Delta_{k_f k_i} = E_{k_f} - E_{k_i}$  is the transition energy between the initial state  $|k_i\rangle$  and the final state  $|k_f\rangle$ . Therefore, the induced electric dipole can be rewritten as

$$\langle \vec{d} \rangle = -\vec{E}_0 \operatorname{Re} \left\{ \sum_{k_i, k_f} \rho_i \left[ \frac{\vec{d}_{k_i, k_f} \vec{d}_{k_f, k_i}}{(\omega - \Delta_{k_f k_i} + i\gamma)} - \frac{\vec{d}_{k_i, k_f} \vec{d}_{k_f, k_i}}{(\omega + \Delta_{k_f k_i} + i\gamma)} \right] e^{-i\omega t} \right\}. \quad (\text{S20})$$

Because of the rotating-wave approximation [S3], the second term of the above equation should be neglected, i.e.

$$\langle \vec{d} \rangle \approx -\vec{E}_0 \operatorname{Re} \left[ \sum_{k_i, k_f} \frac{\rho_i \vec{d}_{k_i, k_f} \vec{d}_{k_f, k_i}}{\omega - \Delta_{k_f k_i} + i\gamma} e^{-i\omega t} \right]. \quad (\text{S21})$$

Assuming that all NV centers are identical, the polarization density reads

$$\vec{P} = \frac{n_0}{\hbar} \langle \vec{d} \rangle, \quad (\text{S22})$$

where  $n_0$  is the number density of the NV centers in diamond.

### III. LORENTZ LOCAL FIELD THEORY

According to Ref. [S4], in closely-packed molecules the polarization of neighboring molecules gives rise to an internal field  $\vec{E}_i$  at any molecule, in addition to the external field  $\vec{E}$ . The internal field is

$$\vec{E}_i = \vec{E}_{\text{near}} - \vec{E}_{\text{mean}}, \quad (\text{S23})$$

where  $\vec{E}_{\text{near}}$  is the actual contribution from the molecules close to the given molecule, and  $\vec{E}_{\text{mean}}$  is the contribution from those molecules treated in an average continuum. As proven in Ref. [S4], in any crystal structure  $\vec{E}_{\text{near}} = 0$  due to symmetry, and thus  $\vec{E}_i = -\vec{E}_{\text{mean}}$ .

By dipole approximation and assuming no net charge in the volume  $V$ , the mean-field contribution is [S4]

$$\vec{E}_{\text{mean}} = -(\epsilon_D - 1)\vec{E} - \frac{1}{3V\epsilon_0} \sum_l \vec{p}_l, \quad (\text{S24})$$

where  $\epsilon_D = 5.7$  [S5] is relative permittivity of diamond, and the second term is summed over all induced molecular electric dipole moments  $\vec{p}_l$  within the volume. Under the weak field approximation, the induced dipole moment is

$$\vec{p}_l = \epsilon_0 \gamma_{\text{mol}} (\vec{E} + \vec{E}_i), \quad (\text{S25})$$

where  $\gamma_{\text{mol}}$  is generally a second-order tensor. Since  $\vec{E}_i = (\epsilon_D - 1)\vec{E} + \vec{P}/(3\epsilon_0)$  [S4, S6], the polarization  $\vec{P} \equiv \sum_l \vec{p}_l/V = n_0 \vec{p}_l$  reads

$$\vec{P} = n_0 \epsilon_0 \gamma_{\text{mol}} (\vec{E} + \vec{E}_i) = n_0 \epsilon_0 \gamma_{\text{mol}} (\epsilon_D \vec{E} + \frac{\vec{P}}{3\epsilon_0}). \quad (\text{S26})$$

Furthermore, using  $\vec{P} = \epsilon_0 \chi_e \vec{E}$  [S4, S6], we have

$$\epsilon_0 \chi_e \vec{E} = n_0 \epsilon_0 \gamma_{\text{mol}} (\epsilon_D + \frac{\chi_e}{3}) \vec{E}, \quad (\text{S27})$$

leading to

$$\chi_e = \frac{n_0 \gamma_{\text{mol}} \epsilon_D}{1 - \frac{1}{3} n_0 \gamma_{\text{mol}}}. \quad (\text{S28})$$

As proven in Sec. SVII, in diamond with NV centers,  $\gamma_{\text{mol}}$  is of the form

$$\gamma_{\text{mol}} = \begin{pmatrix} \eta(\omega)/n_0 & 0 & 0 \\ 0 & 0 & 0 \\ 0 & 0 & 0 \end{pmatrix}, \quad (\text{S29})$$

where  $\eta(\omega)$  is the second part of Eq. (11) in the main text. Therefore, the electric susceptibility is

$$\chi_e = \begin{pmatrix} \frac{3\epsilon_D\eta}{3-\eta} & 0 & 0 \\ 0 & 0 & 0 \\ 0 & 0 & 0 \end{pmatrix}, \quad (\text{S30})$$

and the relative permittivity is

$$\vec{\epsilon}_r = \begin{pmatrix} \epsilon_D(1 + \frac{3\eta}{3-\eta}) & 0 & 0 \\ 0 & \epsilon_D & 0 \\ 0 & 0 & \epsilon_D \end{pmatrix}. \quad (\text{S31})$$

The window of the negative refraction is determined by the two solutions to the equation

$$1 + \frac{3\eta}{3-\eta} = 0, \text{ or equivalently, } \frac{3}{2} + \eta = 0, \quad (\text{S32})$$

which is not qualitatively different from the equation for the case without the local field correction

$$\epsilon_D + \eta = 0. \quad (\text{S33})$$

As a result, both the center and width of the negative refraction domain are not substantially modified by the Lorentz local field correction. This is in consistent with the numerical results in Refs. [S7–S9].

#### SIV. SELECTION RULES OF OPTICAL TRANSITIONS

According to Ref. [S10], there are four outer electrons distributed in the  $a_1$ ,  $e_x$  and  $e_y$  levels, i.e.,  $a_1^2 e^2$ . On account of the spin degree of freedom, the electronic ground states can be written in the second quantization form,  $|a_1 \bar{a}_1 e_x \bar{e}_x e_y \bar{e}_y\rangle$  with an overbar denoting spin-down, as

$$|\Phi_{A_2;1,0}^c\rangle = \frac{1}{\sqrt{2}}(|111001\rangle + |110110\rangle), \quad (\text{S34})$$

$$|\Phi_{A_2;1,1}^c\rangle = |111010\rangle, \quad (\text{S35})$$

$$|\Phi_{A_2;1,-1}^c\rangle = |110101\rangle, \quad (\text{S36})$$

where the superscript  $c$  means configuration, the subscripts are ordered as  $j, k; S, m_s$  with  $j$  being the irreducible representation,  $k$  being the row of irreducible representation,  $S$  being the total spin and  $m_s$  being the spin projection along the symmetry axis of the NV. The six first excited states, i.e.,  $a_1 e^3$ , are respectively

$$|\Phi_{E,x;1,0}^c\rangle = \frac{1}{\sqrt{2}}(|100111\rangle + |011011\rangle), \quad (\text{S37})$$

$$|\Phi_{E,y;1,0}^c\rangle = \frac{1}{\sqrt{2}}(|101101\rangle + |011110\rangle), \quad (\text{S38})$$

$$|\Phi_{E,x;1,1}^c\rangle = |101011\rangle, \quad (\text{S39})$$

$$|\Phi_{E,y;1,1}^c\rangle = |101110\rangle, \quad (\text{S40})$$

$$|\Phi_{E,x;1,-1}^c\rangle = |010111\rangle, \quad (\text{S41})$$

$$|\Phi_{E,y;1,-1}^c\rangle = |011101\rangle. \quad (\text{S42})$$

By comparing the above states, we notice that there is one electron transiting from the  $a_1$  orbital to the  $e$  orbital. In the absence of spin-orbital coupling, on account of conservation of spin and total angular momentum [S11], the

following transitions are allowed by the electric dipole coupling

$$|\Phi_{A_2;1,0}^c\rangle \equiv |\Phi_{E,x;1,0}^c\rangle, |\Phi_{E,y;1,0}^c\rangle, \quad (\text{S43})$$

$$|\Phi_{A_2;1,1}^c\rangle \equiv |\Phi_{E,x;1,1}^c\rangle, |\Phi_{E,y;1,1}^c\rangle, \quad (\text{S44})$$

$$|\Phi_{A_2;1,-1}^c\rangle \equiv |\Phi_{E,x;1,-1}^c\rangle, |\Phi_{E,y;1,-1}^c\rangle. \quad (\text{S45})$$

The non-zero transition matrix elements of the position vector  $\vec{r} = x\hat{e}_x + y\hat{e}_y + z\hat{e}_z$  ( $\hat{e}_i$  unit vector along direction  $i = x, y, z$ ) are listed as [S12]

$$\langle a_1|x|e_x\rangle \neq 0, \quad (\text{S46})$$

$$\langle a_1|y|e_y\rangle \neq 0, \quad (\text{S47})$$

$$\langle e_y|y|e_x\rangle = \langle e_y|x|e_y\rangle = \langle e_x|y|e_y\rangle = -\langle e_x|x|e_x\rangle \neq 0. \quad (\text{S48})$$

Therefore, we have

$$\begin{aligned} \langle \Phi_{A_2;1,0}^c|x|\Phi_{E,x;1,0}^c\rangle &= \frac{1}{\sqrt{2}}(\langle 111001| + \langle 110110|)x\frac{1}{\sqrt{2}}(|100111\rangle + |011011\rangle) \\ &= \frac{1}{2}\langle a_1|x|e_y\rangle + \frac{1}{2}\langle \bar{a}_1|x|\bar{e}_y\rangle = 0, \end{aligned} \quad (\text{S49})$$

$$\begin{aligned} \langle \Phi_{A_2;1,0}^c|y|\Phi_{E,x;1,0}^c\rangle &= \frac{1}{\sqrt{2}}(\langle 111001| + \langle 110110|)y\frac{1}{\sqrt{2}}(|100111\rangle + |011011\rangle) \\ &= \frac{1}{2}\langle a_1|y|e_y\rangle + \frac{1}{2}\langle \bar{a}_1|y|\bar{e}_y\rangle = \langle a_1|y|e_y\rangle, \end{aligned} \quad (\text{S50})$$

$$\begin{aligned} \langle \Phi_{A_2;1,0}^c|x|\Phi_{E,y;1,0}^c\rangle &= \frac{1}{\sqrt{2}}(\langle 111001| + \langle 110110|)x\frac{1}{\sqrt{2}}(|101101\rangle + |011110\rangle) \\ &= \frac{1}{2}\langle \bar{a}_1|x|\bar{e}_x\rangle + \frac{1}{2}\langle a_1|x|e_x\rangle = \langle a_1|x|e_x\rangle, \end{aligned} \quad (\text{S51})$$

$$\begin{aligned} \langle \Phi_{A_2;1,0}^c|y|\Phi_{E,y;1,0}^c\rangle &= \frac{1}{\sqrt{2}}(\langle 111001| + \langle 110110|)y\frac{1}{\sqrt{2}}(|101101\rangle + |011110\rangle) \\ &= \frac{1}{2}\langle \bar{a}_1|y|\bar{e}_x\rangle + \frac{1}{2}\langle a_1|y|e_x\rangle = 0, \end{aligned} \quad (\text{S52})$$

$$\langle \Phi_{A_2;1,1}^c|x|\Phi_{E,x;1,1}^c\rangle = \langle 111010|x|101011\rangle = \langle \bar{a}_1|x|\bar{e}_y\rangle = 0, \quad (\text{S53})$$

$$\langle \Phi_{A_2;1,1}^c|y|\Phi_{E,x;1,1}^c\rangle = \langle 111010|y|101011\rangle = \langle \bar{a}_1|y|\bar{e}_y\rangle, \quad (\text{S54})$$

$$\langle \Phi_{A_2;1,1}^c|x|\Phi_{E,y;1,1}^c\rangle = \langle 111010|x|101110\rangle = \langle \bar{a}_1|x|\bar{e}_x\rangle, \quad (\text{S55})$$

$$\langle \Phi_{A_2;1,1}^c|y|\Phi_{E,y;1,1}^c\rangle = \langle 111010|y|101110\rangle = \langle \bar{a}_1|y|\bar{e}_x\rangle = 0, \quad (\text{S56})$$

$$\langle \Phi_{A_2;1,-1}^c|x|\Phi_{E,x;1,-1}^c\rangle = \langle 110101|x|010111\rangle = \langle a_1|x|e_y\rangle = 0, \quad (\text{S57})$$

$$\langle \Phi_{A_2;1,-1}^c|y|\Phi_{E,x;1,-1}^c\rangle = \langle 110101|y|010111\rangle = \langle a_1|y|e_y\rangle, \quad (\text{S58})$$

$$\langle \Phi_{A_2;1,-1}^c|x|\Phi_{E,y;1,-1}^c\rangle = \langle 110101|x|011101\rangle = \langle a_1|x|e_x\rangle, \quad (\text{S59})$$

$$\langle \Phi_{A_2;1,-1}^c|y|\Phi_{E,y;1,-1}^c\rangle = \langle 110101|y|011101\rangle = \langle a_1|y|e_x\rangle = 0. \quad (\text{S60})$$

To summarize, the selection rules for optical transitions are

$$|\Phi_{A_2;1,0}^c\rangle \underline{\underline{y}} |\Phi_{E,x;1,0}^c\rangle, \quad (\text{S61})$$

$$|\Phi_{A_2;1,0}^c\rangle \underline{\underline{x}} |\Phi_{E,y;1,0}^c\rangle, \quad (\text{S62})$$

$$|\Phi_{A_2;1,1}^c\rangle \underline{\underline{y}} |\Phi_{E,x;1,1}^c\rangle, \quad (\text{S63})$$

$$|\Phi_{A_2;1,1}^c\rangle \underline{\underline{x}} |\Phi_{E,y;1,1}^c\rangle, \quad (\text{S64})$$

$$|\Phi_{A_2;1,-1}^c\rangle \underline{\underline{y}} |\Phi_{E,x;1,-1}^c\rangle, \quad (\text{S65})$$

$$|\Phi_{A_2;1,-1}^c\rangle \underline{\underline{x}} |\Phi_{E,y;1,-1}^c\rangle, \quad (\text{S66})$$

where the label over the arrow indicates the polarization of the electric field. In short,

$$|\Phi_{A_2;S,m_s}^c\rangle_{\alpha'} \alpha' |\Phi_{E,\alpha;S,m_s}^c\rangle, \quad (\text{S67})$$

where  $\alpha, \alpha' = x, y$  and  $\alpha \neq \alpha'$ . In addition,  $|\Phi_{E,x;S,m_s}^c\rangle$  and  $|\Phi_{E,y;S,m_s}^c\rangle$  remain degenerate when applying a magnetic field.

For the electronic ground states, they can be formally diagonalized as

$$|g_i\rangle = \sum_{j=-1}^1 C_{i,j}^g |\Phi_{A_2;1,j}^c\rangle = C_{i,0}^g |\Phi_{A_2;1,0}^c\rangle + C_{i,1}^g |\Phi_{A_2;1,1}^c\rangle + C_{i,-1}^g |\Phi_{A_2;1,-1}^c\rangle, \quad (\text{S68})$$

with eigenenergies  $E_i^g$ . For the electronic excited state, they can be likewise diagonalized in two sets according to their polarizations as

$$|e_i^x\rangle = \sum_{j=-1}^1 C_{i,j}^e |\Phi_{E,x;1,j}^c\rangle = C_{i,0}^e |\Phi_{E,x;1,0}^c\rangle + C_{i,1}^e |\Phi_{E,x;1,1}^c\rangle + C_{i,-1}^e |\Phi_{E,x;1,-1}^c\rangle, \quad (\text{S69})$$

$$|e_i^y\rangle = \sum_{j=-1}^1 C_{i,j}^e |\Phi_{E,y;1,j}^c\rangle = C_{i,0}^e |\Phi_{E,y;1,0}^c\rangle + C_{i,1}^e |\Phi_{E,y;1,1}^c\rangle + C_{i,-1}^e |\Phi_{E,y;1,-1}^c\rangle, \quad (\text{S70})$$

with eigenenergies  $E_i^e$ , where they share the same coefficients due to the degeneracy.

According to Refs. [S4, S13], the constitutive relation reads

$$\vec{D} = \epsilon_0 \overleftrightarrow{\epsilon}_r \vec{E} = \epsilon_D \epsilon_0 \vec{E} + \vec{P}, \quad (\text{S71})$$

where  $\epsilon_0$  is the permittivity of the vacuum,  $\overleftrightarrow{\epsilon}_r$  is the relative permittivity of diamond with NV centers,  $\vec{E}$  is the applied electric field,  $\epsilon_D$  is the relative permittivity of pure diamond, and the polarization density can be calculated by linear response theory [S2] as

$$\begin{aligned} \vec{P} &= -\frac{n_0}{\hbar} \text{Re} \left[ \sum_{j,i,f} \rho_i \frac{\vec{d}_{if}^{(j)} (\vec{d}_{fi}^{(j)} \cdot \vec{E})}{\omega - \Delta_{fi}^{(j)} + i\gamma} \right] \\ &= -\frac{n_0}{3\hbar} \text{Re} \left[ \frac{\vec{d}_{g_1 e_1}^{(j)} (\vec{d}_{e_1 g_1}^{(j)} \cdot \vec{E})}{\omega - \Delta_{e_1 g_1}^{(j)} + i\gamma} + \frac{\vec{d}_{g_1 e_2}^{(j)} (\vec{d}_{e_2 g_1}^{(j)} \cdot \vec{E})}{\omega - \Delta_{e_2 g_1}^{(j)} + i\gamma} + \frac{\vec{d}_{g_1 e_3}^{(j)} (\vec{d}_{e_3 g_1}^{(j)} \cdot \vec{E})}{\omega - \Delta_{e_3 g_1}^{(j)} + i\gamma} \right. \\ &\quad + \frac{\vec{d}_{g_2 e_1}^{(j)} (\vec{d}_{e_1 g_2}^{(j)} \cdot \vec{E})}{\omega - \Delta_{e_1 g_2}^{(j)} + i\gamma} + \frac{\vec{d}_{g_2 e_2}^{(j)} (\vec{d}_{e_2 g_2}^{(j)} \cdot \vec{E})}{\omega - \Delta_{e_2 g_2}^{(j)} + i\gamma} + \frac{\vec{d}_{g_2 e_3}^{(j)} (\vec{d}_{e_3 g_2}^{(j)} \cdot \vec{E})}{\omega - \Delta_{e_3 g_2}^{(j)} + i\gamma} \\ &\quad \left. + \frac{\vec{d}_{g_3 e_1}^{(j)} (\vec{d}_{e_1 g_3}^{(j)} \cdot \vec{E})}{\omega - \Delta_{e_1 g_3}^{(j)} + i\gamma} + \frac{\vec{d}_{g_3 e_2}^{(j)} (\vec{d}_{e_2 g_3}^{(j)} \cdot \vec{E})}{\omega - \Delta_{e_2 g_3}^{(j)} + i\gamma} + \frac{\vec{d}_{g_3 e_3}^{(j)} (\vec{d}_{e_3 g_3}^{(j)} \cdot \vec{E})}{\omega - \Delta_{e_3 g_3}^{(j)} + i\gamma} \right]. \quad (\text{S72}) \end{aligned}$$

Here,  $\vec{d}_{if}^{(j)} = \langle i | \vec{d}^{(j)} | f \rangle$  is the matrix element of electric dipole of  $j$ th NV center between the initial state  $|i\rangle$  and final state  $|f\rangle$ ;  $\Delta_{fi}^{(j)}$  is the transition energy between the initial state  $|i\rangle$  and the final state  $|f\rangle$  of  $j$ th NV center; and  $\gamma$  is the decay rate of the electronic excited state. The summation  $\sum_j$  is over all NV centers within the volume  $v_0 = n_0^{-1}$ , and  $\omega$  is the frequency of the incident light. In the above equation, we did not explicitly discriminate the contributions from  $|e_i^x\rangle$  and  $|e_i^y\rangle$  as they only differ by the polarization direction.

For the transition  $E_1^g(j) \leftrightarrow E_1^e(j)$ , note that

$$\begin{aligned} \frac{\bar{d}_{g_1 e_1}^{(j)}(\bar{d}_{e_1 g_1}^{(j)} \cdot \vec{E})}{\omega - \Delta_{e_1 g_1}^{(j)} + i\gamma} &= \frac{\sum_{j_1, j_2, j_3, j_4} C_{1, j_1}^{g*} C_{1, j_2}^e C_{1, j_3}^{e*} C_{1, j_4}^g \langle \Phi_{A_2; 1, j_1}^c | \bar{d}^{(j)} | \Phi_{E; 1, j_2}^c \rangle \langle \Phi_{E; 1, j_3}^c | \bar{d}^{(j)} | \Phi_{A_2; 1, j_4}^c \rangle \cdot \vec{E}}{\omega - [E_1^e(j) - E_1^g(j)] + i\gamma} \\ &= \frac{\sum_{j_1, j_3} C_{1, j_1}^{g*} C_{1, j_1}^e C_{1, j_3}^{e*} C_{1, j_3}^g \langle \Phi_{A_2; 1, j_1}^c | \bar{d}^{(j)} | \Phi_{E; 1, j_1}^c \rangle \langle \Phi_{E; 1, j_3}^c | \bar{d}^{(j)} | \Phi_{A_2; 1, j_3}^c \rangle \cdot \vec{E}}{\omega - [E_1^e(j) - E_1^g(j)] + i\gamma} \\ &= \frac{\sum_{j_1, j_2} C_{1, j_1}^{g*} C_{1, j_1}^e C_{1, j_2}^{e*} C_{1, j_2}^g}{\omega - [E_1^e(j) - E_1^g(j)] + i\gamma} (\bar{d}_x^{(j)} + \bar{d}_y^{(j)}) (\bar{d}_x^{(j)} + \bar{d}_y^{(j)}) \cdot \vec{E}, \end{aligned} \quad (\text{S73})$$

$$\frac{\bar{d}_{g_1 e_2}^{(j)}(\bar{d}_{e_2 g_1}^{(j)} \cdot \vec{E})}{\omega - \Delta_{e_2 g_1}^{(j)} + i\gamma} = \frac{\sum_{j_1, j_2} C_{1, j_1}^{g*} C_{2, j_1}^e C_{2, j_2}^{e*} C_{1, j_2}^g}{\omega - [E_2^e(j) - E_1^g(j)] + i\gamma} (\bar{d}_x^{(j)} + \bar{d}_y^{(j)}) (\bar{d}_x^{(j)} + \bar{d}_y^{(j)}) \cdot \vec{E}, \quad (\text{S74})$$

$$\frac{\bar{d}_{g_1 e_3}^{(j)}(\bar{d}_{e_3 g_1}^{(j)} \cdot \vec{E})}{\omega - \Delta_{e_3 g_1}^{(j)} + i\gamma} = \frac{\sum_{j_1, j_2} C_{1, j_1}^{g*} C_{3, j_1}^e C_{3, j_2}^{e*} C_{1, j_2}^g}{\omega - [E_3^e(j) - E_1^g(j)] + i\gamma} (\bar{d}_x^{(j)} + \bar{d}_y^{(j)}) (\bar{d}_x^{(j)} + \bar{d}_y^{(j)}) \cdot \vec{E}, \quad (\text{S75})$$

$$\frac{\bar{d}_{g_2 e_1}^{(j)}(\bar{d}_{e_1 g_2}^{(j)} \cdot \vec{E})}{\omega - \Delta_{e_1 g_2}^{(j)} + i\gamma} = \frac{\sum_{j_1, j_2} C_{2, j_1}^{g*} C_{1, j_1}^e C_{1, j_2}^{e*} C_{2, j_2}^g}{\omega - [E_1^e(j) - E_2^g(j)] + i\gamma} (\bar{d}_x^{(j)} + \bar{d}_y^{(j)}) (\bar{d}_x^{(j)} + \bar{d}_y^{(j)}) \cdot \vec{E}, \quad (\text{S76})$$

$$\frac{\bar{d}_{g_2 e_2}^{(j)}(\bar{d}_{e_2 g_2}^{(j)} \cdot \vec{E})}{\omega - \Delta_{e_2 g_2}^{(j)} + i\gamma} = \frac{\sum_{j_1, j_2} C_{2, j_1}^{g*} C_{2, j_1}^e C_{2, j_2}^{e*} C_{2, j_2}^g}{\omega - [E_2^e(j) - E_2^g(j)] + i\gamma} (\bar{d}_x^{(j)} + \bar{d}_y^{(j)}) (\bar{d}_x^{(j)} + \bar{d}_y^{(j)}) \cdot \vec{E}, \quad (\text{S77})$$

$$\frac{\bar{d}_{g_2 e_3}^{(j)}(\bar{d}_{e_3 g_2}^{(j)} \cdot \vec{E})}{\omega - \Delta_{e_3 g_2}^{(j)} + i\gamma} = \frac{\sum_{j_1, j_2} C_{2, j_1}^{g*} C_{3, j_1}^e C_{3, j_2}^{e*} C_{2, j_2}^g}{\omega - [E_3^e(j) - E_2^g(j)] + i\gamma} (\bar{d}_x^{(j)} + \bar{d}_y^{(j)}) (\bar{d}_x^{(j)} + \bar{d}_y^{(j)}) \cdot \vec{E}, \quad (\text{S78})$$

$$\frac{\bar{d}_{g_3 e_1}^{(j)}(\bar{d}_{e_1 g_3}^{(j)} \cdot \vec{E})}{\omega - \Delta_{e_1 g_3}^{(j)} + i\gamma} = \frac{\sum_{j_1, j_2} C_{3, j_1}^{g*} C_{1, j_1}^e C_{1, j_2}^{e*} C_{3, j_2}^g}{\omega - [E_1^e(j) - E_3^g(j)] + i\gamma} (\bar{d}_x^{(j)} + \bar{d}_y^{(j)}) (\bar{d}_x^{(j)} + \bar{d}_y^{(j)}) \cdot \vec{E}, \quad (\text{S79})$$

$$\frac{\bar{d}_{g_3 e_2}^{(j)}(\bar{d}_{e_2 g_3}^{(j)} \cdot \vec{E})}{\omega - \Delta_{e_2 g_3}^{(j)} + i\gamma} = \frac{\sum_{j_1, j_2} C_{3, j_1}^{g*} C_{2, j_1}^e C_{2, j_2}^{e*} C_{3, j_2}^g}{\omega - [E_2^e(j) - E_3^g(j)] + i\gamma} (\bar{d}_x^{(j)} + \bar{d}_y^{(j)}) (\bar{d}_x^{(j)} + \bar{d}_y^{(j)}) \cdot \vec{E}, \quad (\text{S80})$$

$$\frac{\bar{d}_{g_3 e_3}^{(j)}(\bar{d}_{e_3 g_3}^{(j)} \cdot \vec{E})}{\omega - \Delta_{e_3 g_3}^{(j)} + i\gamma} = \frac{\sum_{j_1, j_2} C_{3, j_1}^{g*} C_{3, j_1}^e C_{3, j_2}^{e*} C_{3, j_2}^g}{\omega - [E_3^e(j) - E_3^g(j)] + i\gamma} (\bar{d}_x^{(j)} + \bar{d}_y^{(j)}) (\bar{d}_x^{(j)} + \bar{d}_y^{(j)}) \cdot \vec{E}. \quad (\text{S81})$$

Therefore, the induced dielectric polarization density can be written as

$$\begin{aligned} \vec{P} &= -\frac{n_0}{3\hbar} \text{Re} \left\{ \frac{\sum_{j_1, j_2} C_{1, j_1}^{g*} C_{1, j_1}^e C_{1, j_2}^{e*} C_{1, j_2}^g}{\omega - [E_1^e(j) - E_1^g(j)] + i\gamma} + \frac{\sum_{j_1, j_2} C_{1, j_1}^{g*} C_{2, j_1}^e C_{2, j_2}^{e*} C_{1, j_2}^g}{\omega - [E_2^e(j) - E_1^g(j)] + i\gamma} + \frac{\sum_{j_1, j_2} C_{1, j_1}^{g*} C_{3, j_1}^e C_{3, j_2}^{e*} C_{1, j_2}^g}{\omega - [E_3^e(j) - E_1^g(j)] + i\gamma} \right. \\ &\quad + \frac{\sum_{j_1, j_2} C_{2, j_1}^{g*} C_{1, j_1}^e C_{1, j_2}^{e*} C_{2, j_2}^g}{\omega - [E_1^e(j) - E_2^g(j)] + i\gamma} + \frac{\sum_{j_1, j_2} C_{2, j_1}^{g*} C_{2, j_1}^e C_{2, j_2}^{e*} C_{2, j_2}^g}{\omega - [E_2^e(j) - E_2^g(j)] + i\gamma} + \frac{\sum_{j_1, j_2} C_{2, j_1}^{g*} C_{3, j_1}^e C_{3, j_2}^{e*} C_{2, j_2}^g}{\omega - [E_3^e(j) - E_2^g(j)] + i\gamma} \\ &\quad \left. + \frac{\sum_{j_1, j_2} C_{3, j_1}^{g*} C_{1, j_1}^e C_{1, j_2}^{e*} C_{3, j_2}^g}{\omega - [E_1^e(j) - E_3^g(j)] + i\gamma} + \frac{\sum_{j_1, j_2} C_{3, j_1}^{g*} C_{2, j_1}^e C_{2, j_2}^{e*} C_{3, j_2}^g}{\omega - [E_2^e(j) - E_3^g(j)] + i\gamma} + \frac{\sum_{j_1, j_2} C_{3, j_1}^{g*} C_{3, j_1}^e C_{3, j_2}^{e*} C_{3, j_2}^g}{\omega - [E_3^e(j) - E_3^g(j)] + i\gamma} \right\} \\ &\quad \times (\bar{d}_x^{(j)} + \bar{d}_y^{(j)}) (\bar{d}_x^{(j)} + \bar{d}_y^{(j)}) \cdot \vec{E}. \end{aligned} \quad (\text{S82})$$

As a result, the relative permittivity tensor is

$$\begin{aligned} \overleftrightarrow{\epsilon}_r(\omega) &= \epsilon_D - \frac{n_0}{3\hbar\epsilon_0} \text{Re} \left\{ \frac{\sum_{j_1, j_2} C_{1, j_1}^{g*} C_{1, j_1}^e C_{1, j_2}^{e*} C_{1, j_2}^g}{\omega - [E_1^e(j) - E_1^g(j)] + i\gamma} + \frac{\sum_{j_1, j_2} C_{1, j_1}^{g*} C_{2, j_1}^e C_{2, j_2}^{e*} C_{1, j_2}^g}{\omega - [E_2^e(j) - E_1^g(j)] + i\gamma} + \frac{\sum_{j_1, j_2} C_{1, j_1}^{g*} C_{3, j_1}^e C_{3, j_2}^{e*} C_{1, j_2}^g}{\omega - [E_3^e(j) - E_1^g(j)] + i\gamma} \right. \\ &\quad + \frac{\sum_{j_1, j_2} C_{2, j_1}^{g*} C_{1, j_1}^e C_{1, j_2}^{e*} C_{2, j_2}^g}{\omega - [E_1^e(j) - E_2^g(j)] + i\gamma} + \frac{\sum_{j_1, j_2} C_{2, j_1}^{g*} C_{2, j_1}^e C_{2, j_2}^{e*} C_{2, j_2}^g}{\omega - [E_2^e(j) - E_2^g(j)] + i\gamma} + \frac{\sum_{j_1, j_2} C_{2, j_1}^{g*} C_{3, j_1}^e C_{3, j_2}^{e*} C_{2, j_2}^g}{\omega - [E_3^e(j) - E_2^g(j)] + i\gamma} \\ &\quad \left. + \frac{\sum_{j_1, j_2} C_{3, j_1}^{g*} C_{1, j_1}^e C_{1, j_2}^{e*} C_{3, j_2}^g}{\omega - [E_1^e(j) - E_3^g(j)] + i\gamma} + \frac{\sum_{j_1, j_2} C_{3, j_1}^{g*} C_{2, j_1}^e C_{2, j_2}^{e*} C_{3, j_2}^g}{\omega - [E_2^e(j) - E_3^g(j)] + i\gamma} + \frac{\sum_{j_1, j_2} C_{3, j_1}^{g*} C_{3, j_1}^e C_{3, j_2}^{e*} C_{3, j_2}^g}{\omega - [E_3^e(j) - E_3^g(j)] + i\gamma} \right\} \\ &\quad \times (\bar{d}_x^{(j)} + \bar{d}_y^{(j)}) (\bar{d}_x^{(j)} + \bar{d}_y^{(j)}). \end{aligned} \quad (\text{S83})$$

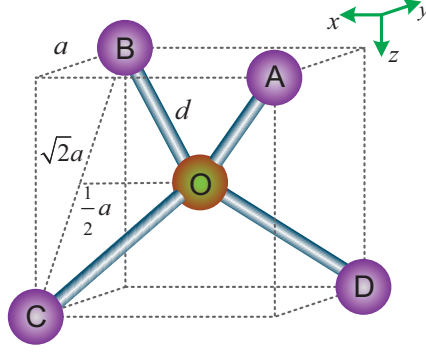


Figure S1. (color online) Four possible orientations of NV centers in diamond [S1, S14]:  $\vec{r}_{OA} = (-1, -1, -1)/\sqrt{3}$ ,  $\vec{r}_{OB} = (1, 1, -1)/\sqrt{3}$ ,  $\vec{r}_{OC} = (1, -1, 1)/\sqrt{3}$ , and  $\vec{r}_{OD} = (-1, 1, 1)/\sqrt{3}$ .  $d = 154$  pm is the length of carbon bond. The side length of the cube is  $a = \frac{2}{\sqrt{3}}d$ . The angle between any pair of the above four orientations is  $109^\circ 28'$ .

Clearly, there may be nine possible negative permittivities around the nine transition frequencies  $\Delta_{e_i g_j}^{(j)} = E_i^e(j) - E_j^g(j)$ .

As shown in Fig. S1, in diamond there are four possible symmetry axes for the NV centers, i.e.  $\vec{r}_{OA} = (-1, -1, -1)/\sqrt{3}$ ,  $\vec{r}_{OB} = (1, 1, -1)/\sqrt{3}$ ,  $\vec{r}_{OC} = (1, -1, 1)/\sqrt{3}$ , and  $\vec{r}_{OD} = (-1, 1, 1)/\sqrt{3}$ . Here,  $\vec{r}_{OA}$  can be obtained by rotating the  $z$ -axis around the axis  $\vec{n}_{OA} = (-1, 1, 0)/\sqrt{2}$  by an angle  $\theta_{OA} = -(180^\circ - 109^\circ 28'/2) = -125^\circ 16'$ , i.e.,

$$\vec{r}_{OA} = R(\vec{n}_{OA}, \theta_{OA})\hat{e}_z = R(\vec{n}_{OA}, \theta_{OA})(0, 0, 1)^T, \quad (\text{S84})$$

where the rotation matrix around  $\vec{n} = (n_x, n_y, n_z)$  with an angle  $\theta$  is [S15]

$$R(\vec{n}, \theta) = \begin{pmatrix} \cos \theta + n_x^2(1 - \cos \theta) & n_x n_y(1 - \cos \theta) - n_z \sin \theta & n_x n_z(1 - \cos \theta) + n_y \sin \theta \\ n_x n_y(1 - \cos \theta) + n_z \sin \theta & \cos \theta + n_y^2(1 - \cos \theta) & n_y n_z(1 - \cos \theta) - n_x \sin \theta \\ n_x n_z(1 - \cos \theta) - n_y \sin \theta & n_y n_z(1 - \cos \theta) + n_x \sin \theta & \cos \theta + n_z^2(1 - \cos \theta) \end{pmatrix}. \quad (\text{S85})$$

And  $\vec{r}_{OB}$  can be obtained by rotating the  $z$ -axis around the axis  $\vec{n}_{OA} = (-1, 1, 0)/\sqrt{2}$  by an angle  $-\theta_{OA} = 125^\circ 16'$ , i.e.,

$$\vec{r}_{OB} = R(\vec{n}_{OA}, -\theta_{OA})\hat{e}_z. \quad (\text{S86})$$

And  $\vec{r}_{OC}$  can be obtained by rotating the  $z$ -axis around the axis  $\vec{n}_{OC} = (1, 1, 0)/\sqrt{2}$  by an angle  $\theta_{OC} = 109^\circ 28'/2 = 54^\circ 44'$ , i.e.,

$$\vec{r}_{OC} = R(\vec{n}_{OC}, \theta_{OC})\hat{e}_z. \quad (\text{S87})$$

And  $\vec{r}_{OD}$  can be obtained by rotating the  $z$ -axis around the axis  $\vec{n}_{OC} = (1, 1, 0)/\sqrt{2}$  by an angle  $-\theta_{OC} = -54^\circ 44'$ , i.e.,

$$\vec{r}_{OD} = R(\vec{n}_{OC}, -\theta_{OC})\hat{e}_z. \quad (\text{S88})$$

## SV. QUANTUM SWITCH OF NEGATIVE REFRACTION AND NORMAL REFRACTION

As implied by Eq. (S83), the permittivity might be negative around the transition frequencies. In order to switch on/off the negative refraction, we analyze the effect of the magnetic field on the transition frequencies. As shown in Fig. S2, there are generally nine transition frequencies  $\Delta_{ij} = E_i^e - E_j^g$ , which can be subtly tuned by varying the magnetic field.

Below, we analyze the NV center at some specific magnetic fields:

(a) When the magnetic field is absent, the Hamiltonians of the electronic ground state and excited state are respectively simplified as

$$H_{\text{gs}} = D_{\text{gs}} \sum_{m_s = \pm 1} |\Phi_{A_2; 1, m_s}^c\rangle \langle \Phi_{A_2; 1, m_s}^c|, \quad (\text{S89})$$

$$H_{\text{es}} = \sum_{\alpha = x, y} [D_{\text{es}}^\parallel (|\Phi_{E, \alpha; 1, +1}^c\rangle \langle \Phi_{E, \alpha; 1, +1}^c| + |\Phi_{E, \alpha; 1, -1}^c\rangle \langle \Phi_{E, \alpha; 1, -1}^c|) - \xi |\Phi_{E, \alpha; 1, -1}^c\rangle \langle \Phi_{E, \alpha; 1, -1}^c| + \text{h.c.}]. \quad (\text{S90})$$

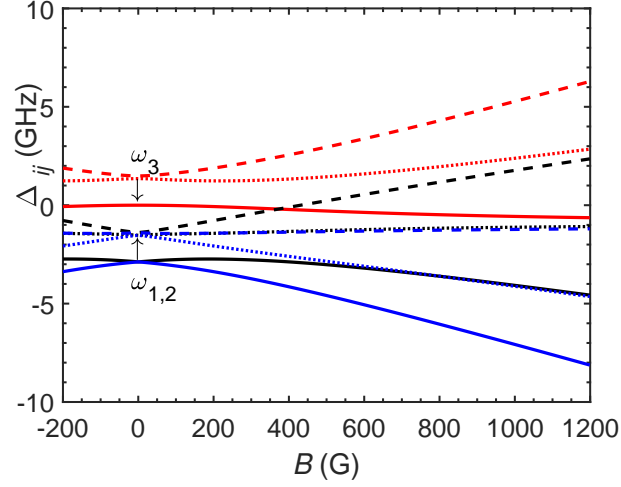


Figure S2. The transition frequencies  $\Delta_{ij} = E_i^e - E_j^g$  versus the magnetic field  $B$ . The magnetic field is applied along the  $z$ -axis. This figure is identical for all four possible orientations of the NV centers due to the special choice of  $\vec{B} \parallel \vec{e}_z$ .

The eigenstates of the electronic ground state are

$$|g_1\rangle = |\Phi_{A_2;1,0}^c\rangle, \quad (\text{S91})$$

$$|g_2\rangle = |\Phi_{A_2;1,+1}^c\rangle, \quad (\text{S92})$$

$$|g_3\rangle = |\Phi_{A_2;1,-1}^c\rangle, \quad (\text{S93})$$

with eigenenergies

$$E_1^g = 0, \quad (\text{S94})$$

$$E_2^g = D_{\text{gs}}, \quad (\text{S95})$$

$$E_3^g = D_{\text{gs}}. \quad (\text{S96})$$

The eigenstates of the electronic excited state are

$$|e_1^\alpha\rangle = |\Phi_{E,\alpha;S,0}^c\rangle, \quad (\text{S97})$$

$$|e_2^\alpha\rangle = (|\Phi_{E,\alpha;S,+1}^c\rangle + |\Phi_{E,\alpha;S,-1}^c\rangle)/\sqrt{2}, \quad (\text{S98})$$

$$|e_3^\alpha\rangle = (|\Phi_{E,\alpha;S,+1}^c\rangle - |\Phi_{E,\alpha;S,-1}^c\rangle)/\sqrt{2}, \quad (\text{S99})$$

with eigenenergies

$$E_1^e = 0, \quad (\text{S100})$$

$$E_2^e = D_{\text{es}}^\parallel + \xi, \quad (\text{S101})$$

$$E_3^e = D_{\text{es}}^\parallel - \xi. \quad (\text{S102})$$

Because the spin is conserved, the following optical transitions are allowed

$$|g_1\rangle \rightleftharpoons |e_1\rangle, \quad (\text{S103})$$

$$|g_2\rangle, |g_3\rangle \rightleftharpoons |e_2\rangle, |e_3\rangle. \quad (\text{S104})$$

These correspond to five peaks around the transition frequencies  $\Delta_{11}$ ,  $\Delta_{22}$ ,  $\Delta_{23}$ ,  $\Delta_{32}$ , and  $\Delta_{33}$ . Furthermore, because  $|g_2\rangle$  and  $|g_3\rangle$  are degenerate,  $\Delta_{22} = \Delta_{23} = D_{\text{es}}^\parallel - D_{\text{gs}} + \xi$  and  $\Delta_{32} = \Delta_{33} = D_{\text{es}}^\parallel - D_{\text{gs}} - \xi$ . Since the separations between the latter four peaks are  $2\xi$ , which is, of the order of GHz, much smaller than the width of the peaks. In Fig. S3, we plot the permittivity for different values of the magnetic field  $B$  and density  $n_0$  of NV centers. Therefore, we would only observe two dips for  $B = 0$ , as shown in Fig. S3(a). Moreover, when the frequency is larger than



$\Delta\omega = 2.37$  GHz, the permittivity becomes positive and thus negative refraction disappears. When the density is increased to  $n_0 = 16$  ppm, cf. Fig. S3(d), the two negative dips remains but the windows on the right is significantly broadened.

(b) When  $B = 514$  G, the electronic excited state is at the avoided crossing point. Correspondingly, the Hamiltonians for the electronic ground and excited states are, respectively, given by

$$H_{\text{es}} \simeq \begin{pmatrix} 2D_{\text{es}}^{\parallel} & D_{\text{es}}^{\parallel}e^{-i\phi} & 0 \\ D_{\text{es}}^{\parallel}e^{i\phi} & 0 & D_{\text{es}}^{\parallel}e^{-i\phi} \\ 0 & D_{\text{es}}^{\parallel}e^{i\phi} & 0 \end{pmatrix}, \quad (\text{S105})$$

$$H_{\text{gs}} \simeq \begin{pmatrix} \frac{3}{2}D_{\text{gs}} & \frac{1}{2}D_{\text{gs}}e^{-i\phi} & 0 \\ \frac{1}{2}D_{\text{gs}}e^{i\phi} & 0 & \frac{1}{2}D_{\text{gs}}e^{-i\phi} \\ 0 & \frac{1}{2}D_{\text{gs}}e^{i\phi} & \frac{1}{2}D_{\text{gs}} \end{pmatrix}. \quad (\text{S106})$$

Since the couplings are comparable to the detunings, the eigenstates in both manifolds effectively mix all three components, i.e.,  $|g_j\rangle = \sum_{m_z} a_{m_z} |\Phi_{A_2;1,m_z}^c\rangle$ ,  $|e_3^{\alpha}\rangle = \sum_{m_z} b_{m_z} |\Phi_{E,\alpha;S,m_z}^c\rangle$ . In this case, we would expect nine possible negative dips at nine transition frequencies. In Fig. S3(b), we observe 7 dips because the degeneracy has been partially broken and there are still two sets of degenerate states. As compared to Fig. S3(a), there is an additional negative dip at  $\Delta\omega = 3.11$  GHz.

(c) When  $B = 1025$  G, there are three additional negative dips at  $\Delta\omega = -4.06$  GHz,  $\Delta\omega = 2.53$  GHz, and  $\Delta\omega = 5.51$  GHz beyond the domain  $[-1.46, 2.37]$  GHz.

## SVI. NEGATIVE REFRACTION AT INTERFACE

By numerical simulation, we have shown that one principle component of the permittivity can be negative while the other principle components remain unchanged. In this section, we will analytically prove that negative refraction can occur at the interface for a transverse magnetic (TH) mode, as shown in Fig. S4. According to Maxwell's equation [S4, S13],

$$\nabla \times \vec{E} = -\frac{\partial}{\partial t} \vec{B} = -\frac{\partial}{\partial t} \mu_0 \vec{H}, \quad (\text{S107})$$

$$\nabla \times \vec{H} = \frac{\partial}{\partial t} \vec{D} = \frac{\partial}{\partial t} \overleftrightarrow{\epsilon} \vec{E}, \quad (\text{S108})$$

$$\nabla \cdot \vec{D} = 0, \quad (\text{S109})$$

$$\nabla \cdot \vec{B} = 0, \quad (\text{S110})$$

where we have assumed  $\vec{J} = 0$  and  $\rho = 0$ ,  $\overleftrightarrow{\epsilon}$  is the permittivity of diamond with NV centers,  $\mu_0$  is the permeability of vacuum and pure diamond.

Assuming that the electric and magnetic fields of the transmitted wave are respectively

$$\vec{E}_t(\vec{r}, t) = (E_{tx}\hat{e}_x + E_{tz}\hat{e}_z) \exp \left[ i(\vec{k}_t \cdot \vec{r} - \omega t) \right], \quad (\text{S111})$$

$$\vec{H}_t(\vec{r}, t) = H_{ty}\hat{e}_y \exp \left[ i(\vec{k}_t \cdot \vec{r} - \omega t) \right], \quad (\text{S112})$$

where  $\vec{k}_t$  and  $\omega$  are respectively the wavevector and frequency of the transmitted wave, we have

$$\nabla \times \vec{E} = i\omega\mu_0 \vec{H}, \quad (\text{S113})$$

$$\nabla \times \vec{H} = -i\omega \overleftrightarrow{\epsilon} \vec{E}. \quad (\text{S114})$$

By inserting Eq. (S114) into Eq. (S113), we have

$$\begin{aligned} \nabla \times \nabla \times \vec{E} &= i\omega\mu_0 \nabla \times \vec{H} \\ &= \overleftrightarrow{\epsilon} \mu_0 \omega^2 \vec{E}. \end{aligned} \quad (\text{S115})$$

This is equivalent to

$$(\nabla \times \nabla \times \overleftrightarrow{I} - \overleftrightarrow{\epsilon} \mu_0 \omega^2) \vec{E} = 0, \quad (\text{S116})$$

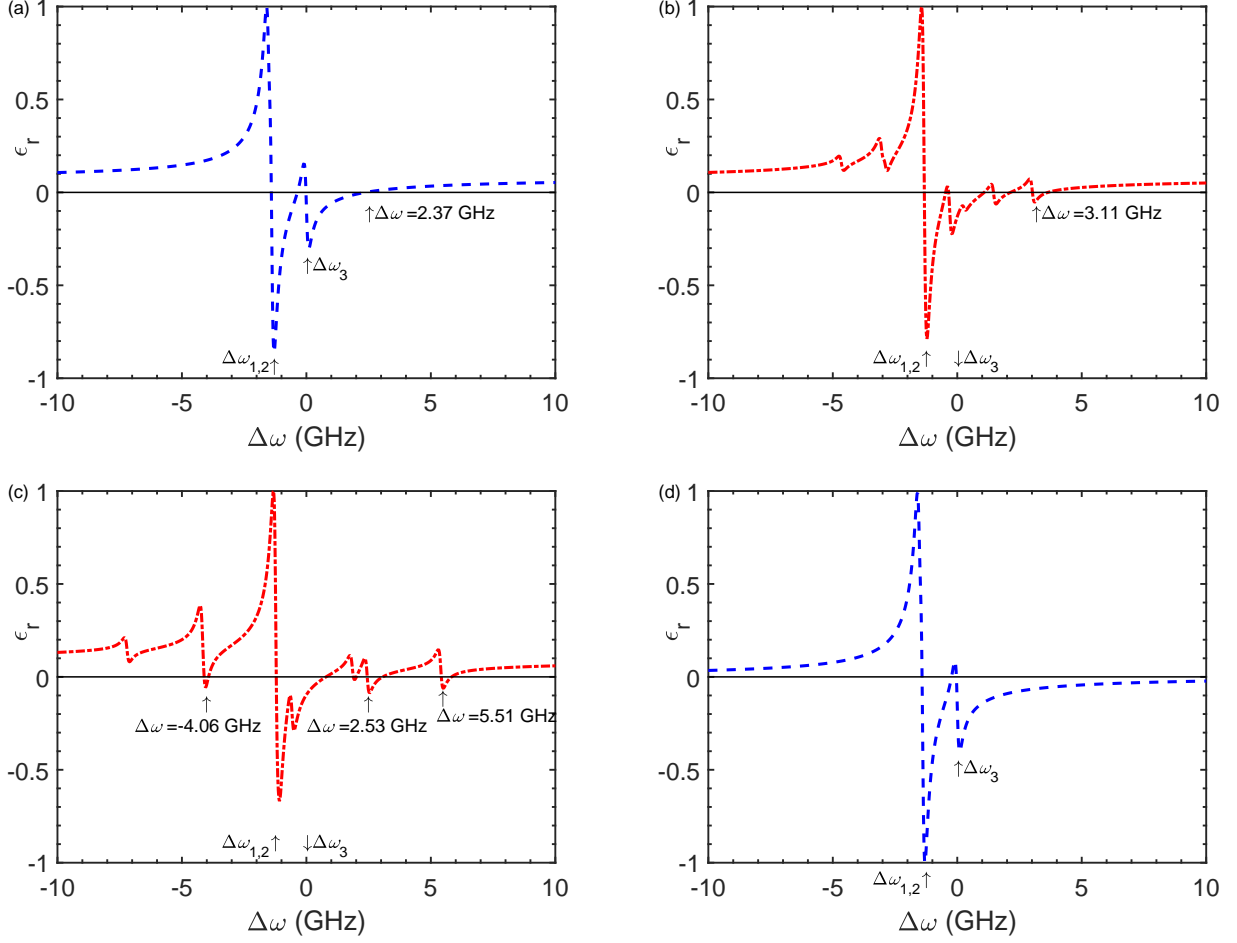


Figure S3. (color online) The frequency dependence of the electric permittivity  $\overleftrightarrow{\epsilon}_r$  of diamond with NV centers for different values of the magnetic field  $B$  and density of NV centers  $n_0$ : (a)  $B_z = 0$  G and  $n_0 = 0.5$  ppm, (b)  $B_z = 514$  G and  $n_0 = 0.5$  ppm, (c)  $B_z = 1025$  G and  $n_0 = 0.5$  ppm, (d)  $B_z = 0$  G and  $n_0 = 16$  ppm. Other parameters are  $d_x = d_y = 11$  D [S16],  $\gamma^{-1} = 10$  ns [S17],  $\epsilon_D = 5.7$  [S5], and  $\mu_D = 1 - 2.1 \times 10^{-5}$  [S18],  $B_x = B_y = 0$  G. The thin black line  $\epsilon_r = 0$  is just a guide to the eye.

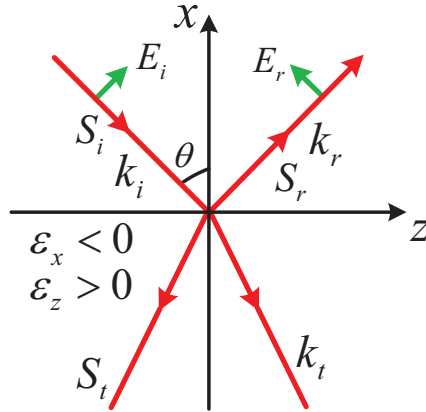


Figure S4. (color online) Negative refraction for hyperbolic dispersion with  $\epsilon_x < 0$  and  $\epsilon_z > 0$ . The TH mode is incident on the interface with electric field  $\vec{E}_i$ , wavevector  $\vec{k}_i$ , Poynting vector  $\vec{S}_i$ , and angle  $\theta$ . It is reflected with electric field  $\vec{E}_r$ , wavevector  $\vec{k}_r$ , and Poynting vector  $\vec{S}_r$ . The Poynting vector, wavevector, electric and magnetic fields of the transmitted wave are respectively  $\vec{S}_t$ ,  $\vec{k}_t$ ,  $\vec{E}_t$ , and  $\vec{H}_t$ .

where  $\overleftrightarrow{I}$  is the identity dyadic. For nontrivial solutions, the determinant of the dyadic should be zero, i.e.

$$\det \begin{pmatrix} \mu_0 \epsilon_x \omega^2 - k_y^2 - k_z^2 & k_x k_y & k_x k_z \\ k_x k_y & \mu_0 \epsilon_y \omega^2 - k_x^2 - k_z^2 & k_y k_z \\ k_x k_z & k_y k_z & \mu_0 \epsilon_z \omega^2 - k_x^2 - k_y^2 \end{pmatrix} = 0, \quad (\text{S117})$$

or equivalently

$$\mu_0 \omega^2 \{ k_x^2 [k_y^2 (\epsilon_x + \epsilon_y) + k_z^2 (\epsilon_x + \epsilon_z) - \mu \omega^2 \epsilon_x (\epsilon_y + \epsilon_z)] + [\epsilon_z (k_z^2 - \mu \omega^2 \epsilon_y) + k_y^2 \epsilon_y] (k_y^2 + k_z^2 - \mu \omega^2 \epsilon_x) + k_x^4 \epsilon_x \} = 0, \quad (\text{S118})$$

where

$$\overleftrightarrow{\epsilon} = \begin{pmatrix} \epsilon_x & 0 & 0 \\ 0 & \epsilon_y & 0 \\ 0 & 0 & \epsilon_z \end{pmatrix}. \quad (\text{S119})$$

The dispersion relations for the ordinary and extraordinary modes are respectively

$$k_x^2 + k_z^2 - \mu_0 \omega^2 \epsilon_y = 0, \quad (\text{S120})$$

$$\epsilon_x k_x^2 + \epsilon_z k_z^2 - \mu_0 \omega^2 \epsilon_x \epsilon_z = 0, \quad (\text{S121})$$

where we have assumed  $k_y = 0$ .

According to the boundary condition [S19], the tangential components of the wavevector across the interface should be equal, i.e.

$$k_{tz} = k_{iz} > 0, \quad (\text{S122})$$

$$k_{ty} = k_{iy}. \quad (\text{S123})$$

By inserting Eq. (S121) into Eq. (S116), we obtain the relation between  $E_{tx}$  and  $E_{tz}$  as

$$\epsilon_x k_{tx} E_{tx} + \epsilon_z k_{tz} E_{tz} = 0. \quad (\text{S124})$$

Using Eq. (S113), we have

$$\begin{aligned} \vec{H} &= \frac{\nabla \times \vec{E}_t}{i\omega\mu_0} \\ &= \frac{\vec{k}_t \times \vec{E}_t}{\omega\mu_0} \\ &= \frac{k_{tz} E_{tx} - k_{tx} E_{tz}}{\omega\mu_0} \hat{e}_y e^{i(\vec{k}_t \cdot \vec{r} - \omega t)} \\ &= \frac{1}{\omega\mu_0} \left( -k_{tz} \frac{\epsilon_z k_{tz} E_{tz}}{\epsilon_x k_{tx}} - k_{tx} E_{tz} \right) \hat{e}_y e^{i(\vec{k}_t \cdot \vec{r} - \omega t)} \\ &= \frac{E_{tz}}{\omega\mu_0} \left( -\frac{\epsilon_z k_{tz}^2 + \epsilon_x k_{tx}^2}{\epsilon_x k_{tx}} \right) \hat{e}_y e^{i(\vec{k}_t \cdot \vec{r} - \omega t)} \\ &= -\frac{E_{tz}}{\omega\mu_0} \frac{\mu_0 \omega^2 \epsilon_x \epsilon_z}{\epsilon_x k_{tx}} \hat{e}_y e^{i(\vec{k}_t \cdot \vec{r} - \omega t)} \\ &= -\frac{\omega \epsilon_z E_{tz}}{k_{tx}} \hat{e}_y e^{i(\vec{k}_t \cdot \vec{r} - \omega t)}. \end{aligned} \quad (\text{S125})$$

The time-averaged Poynting vector of the transmitted wave reads

$$\vec{S}_t = \frac{1}{2} \text{Re}(\vec{E}_t \times \vec{H}_t^*), \quad (\text{S126})$$

with the components being

$$\begin{aligned}
S_{tx} &= \frac{1}{2} \text{Re}(E_{ty}H_{tz}^* - E_{tz}H_{ty}^*) \\
&= -\frac{1}{2} \text{Re}(E_{tz}H_{ty}^*) \\
&= -\frac{1}{2} E_{tz} \left( -\frac{\omega \epsilon_z E_{tz}}{k_{tx}} \right) \\
&= \frac{\omega \epsilon_z}{2k_{tx}} E_{tz}^2,
\end{aligned} \tag{S127}$$

$$\begin{aligned}
S_{tz} &= \frac{1}{2} \text{Re}(E_{tx}H_{ty}^* - E_{ty}H_{tx}^*) \\
&= \frac{1}{2} \text{Re}(E_{tx}H_{ty}^*) \\
&= \frac{1}{2} E_{tx} \left( -\frac{\omega \epsilon_z E_{tz}}{k_{tx}} \right) \\
&= \frac{1}{2} E_{tx} \left( -\frac{\omega \epsilon_z}{k_{tx}} \right) \left( -\frac{\epsilon_x k_{tx} E_{tx}}{\epsilon_y k_{tz}} \right) \\
&= \frac{\epsilon_x \omega E_{tx}^2}{2k_{tz}} < 0,
\end{aligned} \tag{S128}$$

because  $\epsilon_x < 0$ , and  $\omega, k_{tz} > 0$ . In order to transmit energy from the interface into the medium,  $S_{tx}$  should also be negative, and thus  $k_{tx} < 0$  as  $\omega, \epsilon_z > 0$ . Together with Eq. (S121), we have

$$\begin{aligned}
k_{tx} &= \sqrt{\mu_0 \omega^2 \epsilon_z - \frac{\epsilon_z}{\epsilon_x} k_{tz}^2} \\
&= \sqrt{\mu_0 \omega^2 \epsilon_z - \frac{\epsilon_z}{\epsilon_x} k_{iz}^2} \\
&= \sqrt{\mu_0 \omega^2 \epsilon_z - \frac{\epsilon_z}{\epsilon_x} k_i^2 \sin^2 \theta} \\
&= \sqrt{\mu_0 \omega^2 \epsilon_z \left( 1 - \frac{\epsilon_0}{\epsilon_x} \sin^2 \theta \right)},
\end{aligned} \tag{S129}$$

where

$$k_i^2 = \mu_0 \omega^2 \epsilon_0. \tag{S130}$$

## SVII. ANALYSIS OF EXPERIMENTAL FEASIBILITY

According to Refs. [S4, S13], the constitutive relation reads

$$\vec{D} = \epsilon_D \epsilon_0 \vec{E} + \vec{P}, \tag{S131}$$

$$\vec{B} = \mu_0 \vec{H} + \mu_0 \vec{M}, \tag{S132}$$

where  $\epsilon_D$  and  $\mu_0$  are, respectively, the permittivity and permeability of diamond without NV centers,  $\vec{E}$  and  $\vec{B}$  are respectively the electric and magnetic fields with frequency  $\omega$ , the electric polarization and magnetization are respectively

$$\vec{P} = -\frac{n_0}{\hbar} \text{Re} \sum_{j,i,f} \rho_i \frac{\vec{d}_{if} (\vec{d}_{fi} \cdot \vec{E})}{\omega - \Delta_{fi} + i\gamma}, \tag{S133}$$

$$\vec{M} = -\frac{\mu_0 n_0}{\hbar} \text{Re} \sum_{j,i,f} \rho_i \frac{\vec{m}_{if} (\vec{m}_{fi} \cdot \vec{H})}{\omega - \Delta_{fi} + i\gamma}. \tag{S134}$$

Here  $\vec{d}_{if} = \langle i|\vec{d}|f\rangle$  is the matrix element of electric dipole between the initial state  $|i\rangle$  and the final state  $|f\rangle$ ;  $\sum_j$  is the summation over all NV centers within the volume  $v_0$ .  $\Delta_{fi}$  is the transition frequency between the initial and final states;  $\gamma$  is the homogeneous lifetime of all excited states; In the summation the initial and final states should be different,  $i \neq f$ . And the system is initially in a state with density matrix  $\rho(0) = \sum_i \rho_i |i\rangle\langle i|$ .

When there is no magnetic field, the Hamiltonians of the electronic ground and excited states are respectively simplified as

$$H_{\text{gs}} = D_{\text{gs}} S_z^2 = D_{\text{gs}} \sum_{m_z=\pm 1} |\Phi_{A_2;1,m_s}^c\rangle\langle\Phi_{A_2;1,m_s}^c| \quad (\text{S135})$$

$$H_{\text{es}} = D_{\text{es}}^{\parallel} S_z^2 + \xi(S_y^2 - S_x^2) \simeq \sum_{\alpha} D_{\text{es}}^{\parallel} \sum_{m_z=\pm 1} |\Phi_{E,\alpha;1,m_s}^c\rangle\langle\Phi_{E,\alpha;1,m_s}^c|, \quad (\text{S136})$$

where we have dropped the interaction term in order to roughly estimate the minimum density of NV centers in order to realize negative refraction.

The selection rule of optical transition is summarized as [S17]  $|\Phi_{A_2;S,m_s}^c\rangle\langle\Phi_{E,\alpha;S,m_s}^c|$ , where  $m_s = 0, \pm 1$ , both  $S$  and  $m_s$  are conserved. The transition electric dipole has been experimentally estimated as 11 D [S16]. In order to qualitatively estimate the minimum density of NV centers for realizing negative refraction, without loss of generality, the orientations of all NV centers are assumed to be along the  $z$ -axis. Thus, all of the matrix elements of the transition electric dipole are equal

$$\langle\Phi_{E,\alpha;1,m_s}^c|\vec{d}|\Phi_{A_2;1,m_s}^c\rangle = 11(\hat{e}_x + \hat{e}_y)D. \quad (\text{S137})$$

For a specific NV center,  $\hat{e}_z$  should be replaced by the orientation of its principle axis in the lab coordinate system, i.e.,  $\vec{r}_{\text{AO}}$ ,  $\vec{r}_{\text{BO}}$ ,  $\vec{r}_{\text{CO}}$ , and  $\vec{r}_{\text{DO}}$ . Initially, the NV center is in the state

$$\rho(0) = \frac{1}{3} \sum_{m_s=0,\pm 1} |\Phi_{A_2;1,m_s}^c\rangle\langle\Phi_{A_2;1,m_s}^c|. \quad (\text{S138})$$

Therefore,

$$\sum_{i,f} \vec{d}_{if} \vec{d}_{fi} = \frac{4}{3} \times 121 \times (\hat{e}_x \hat{e}_x + \hat{e}_y \hat{e}_y + \hat{e}_x \hat{e}_y + \hat{e}_y \hat{e}_x) D^2, \quad (\text{S139})$$

$$\begin{aligned} \vec{P} &= -\frac{n_0}{\hbar} \text{Re} \sum_{j,i,f} \rho_i \frac{\vec{d}_{if} (\vec{d}_{fi} \cdot \vec{E})}{\omega - \Delta_{fi} + i\gamma} \\ &= -2\epsilon_0 \zeta \gamma \text{Re} \frac{(\hat{e}_x \hat{e}_x + \hat{e}_y \hat{e}_y + \hat{e}_x \hat{e}_y + \hat{e}_y \hat{e}_x) \vec{E}}{\omega - \Delta_{fi} + i\gamma}, \end{aligned} \quad (\text{S140})$$

$$\zeta = \frac{242n_0 D^2}{9\hbar\gamma\epsilon_0}, \quad (\text{S141})$$

where  $\gamma^{-1} = 10$  ns [S17],  $\epsilon_D = 5.7$  [S5] and  $\mu_D = 1 - 2.1 \times 10^{-5}$  [S18] are the relative permittivity and permeability of the pure diamond. For the diamond with NV centers, the electric displacement is

$$\begin{aligned} \vec{D} &= \epsilon_D \epsilon_0 \vec{E} + \vec{P} \\ &= \left[ \epsilon_D - 2\zeta \gamma \text{Re} \frac{(\hat{e}_x \hat{e}_x + \hat{e}_y \hat{e}_y + \hat{e}_x \hat{e}_y + \hat{e}_y \hat{e}_x)}{\omega - \Delta_{fi} + i\gamma} \right] \epsilon_0 \vec{E} \\ &= \left[ \epsilon_D - 2\zeta \gamma \frac{(\omega - \Delta_{fi})(\hat{e}_x \hat{e}_x + \hat{e}_y \hat{e}_y + \hat{e}_x \hat{e}_y + \hat{e}_y \hat{e}_x)}{(\omega - \Delta_{fi})^2 + \gamma^2} \right] \epsilon_0 \vec{E} \\ &\geq \left[ \epsilon_D - 2\zeta \gamma \frac{(\hat{e}_x \hat{e}_x + \hat{e}_y \hat{e}_y + \hat{e}_x \hat{e}_y + \hat{e}_y \hat{e}_x)}{2\gamma} \right] \epsilon_0 \vec{E} \end{aligned} \quad (\text{S142})$$

and thus the tensor of relative permittivity is

$$\overleftrightarrow{\epsilon}_r = \begin{pmatrix} \epsilon_D - \zeta & -\zeta & 0 \\ -\zeta & \epsilon_D - \zeta & 0 \\ 0 & 0 & \epsilon_D \end{pmatrix} \quad (\text{S143})$$

with three principal components being  $\epsilon_r^{(1)} = \epsilon_D - 2\zeta$ , and  $\epsilon_r^{(2)} = \epsilon_r^{(3)} = \epsilon_D$ . In order to make  $\epsilon_r^{(1)} = 0$ , the critical density of the NV centers is

$$n_0^c = \frac{9\hbar\gamma\epsilon_D}{\epsilon_0 \times 484 D^2} = 1.77 \times 10^{21} \text{ m}^{-3}. \quad (\text{S144})$$

Because as shown in Fig. S1 two carbon atoms occupy the volume

$$v = \left( \frac{2}{\sqrt{3}} d \right)^3 = (1.78 \times 10^{-10})^3 \text{ m}^3, \quad (\text{S145})$$

the minimum density of the NV centers to achieve negative refraction is

$$\frac{1}{2} v n_0^c = 5.00 \text{ ppb}, \quad (\text{S146})$$

which is within the range of experimental fabrication, e.g. 16 ppm [S20].

For the NV center with the symmetry axis along  $\vec{r}_{\text{OA}}$ , the principal axis of the negative permittivity is along  $R(\vec{n}_{\text{OA}}, \theta_{\text{OA}})(\vec{e}_x + \vec{e}_y)/\sqrt{2}$ . For the NV center with the symmetry axis along  $\vec{r}_{\text{OB}}$ , the principal axis of the negative permittivity is along  $R(\vec{n}_{\text{OA}}, -\theta_{\text{OA}})(\vec{e}_x + \vec{e}_y)/\sqrt{2}$ . For a medium with the above two orientations, the principal axis of the negative permittivity is along the  $z$ -axis. In the same way, we can prove that for a medium with the other two orientations, i.e. the symmetry axis along  $\vec{r}_{\text{OC}}$  and  $\vec{r}_{\text{OD}}$ , the principal axis of the negative permittivity is also along the  $z$ -axis. Therefore, for the diamond with NV centers along the four possible orientations, the principal axis of the negative permittivity is along the  $z$ -axis.

- 
- [S1] M. W. Doherty, N. B. Manson, P. Delaney, F. Jelezko, J. Wrachtrup, and L. C. L. Hollenberg, The nitrogen-vacancy colour centre in diamond, *Phys. Rep.* **528**, 1 (2013).
- [S2] R. Kubo, M. Toda, and N. Hashitsume, *Statistical Physics II Nonequilibrium Statistical Mechanics* (Springer-Verlag, Berlin Heidelberg, 1985).
- [S3] Q. Ai, Y. Li, H. Zheng, and C. P. Sun, Quantum anti-Zeno effect without rotating wave approximation, *Phys. Rev. A* **81**, 042116 (2010).
- [S4] J. D. Jackson, *Classical Electrodynamics* 3rd ed., (John Wiley, United States, 1999).
- [S5] J. Fontanella, R. L. Johnston, J. H. Colwell, and C. Andeen, Temperature and pressure variation of the refractive index of diamond, *Appl. Opt.* **16**, 2949 (1977).
- [S6] R. Marqués, F. Martín, and M. Sorolla, *Metamaterials with Negative Parameters: Theory, Design and Microwave Applications* (John Wiley, New Jersey, 2008).
- [S7] J. Kästel, M. Fleischhauer, S. F. Yelin, and R. L. Walsworth, Tunable negative refraction without absorption via electromagnetically induced chirality, *Phys. Rev. Lett.* **99**, 073602 (2007).
- [S8] J. Kästel, M. Fleischhauer, and G. Juzeliūnas, Local-field effects in magnetodielectric media: Negative refraction and absorption reduction, *Phys. Rev. A* **76**, 062509 (2007).
- [S9] Y. N. Fang, Y. Shen, Q. Ai, and C. P. Sun, Negative refraction in Möbius molecules, *Phys. Rev. A* **94**, 043805 (2016).
- [S10] M. W. Doherty, N. B. Manson, P. Delaney, and L. C. L. Hollenberg, The negatively charged nitrogen-vacancy centre in diamond: the electronic solution, *New J. Phys.* **13**, 025019 (2011).
- [S11] E. Togan, Y. Chu, A. S. Trifonov, L. Jiang, J. Maze, L. Childress, M. V. G. Dutt, A. S. Sørensen, P. R. Hemmer, A. S. Zibrov, and M. D. Lukin, Quantum entanglement between an optical photon and a solid-state spin qubit, *Nature* **466**, 730 (2010).
- [S12] J. R. Maze, A. Gali, E. Togan, Y. Chu, A. Trifonov, E. Kaxiras, and M. D. Lukin, Properties of nitrogen-vacancy centers in diamond: the group theoretic approach, *New J. Phys.* **13**, 025025 (2011).
- [S13] L. D. Landau, E. M. Lifshitz, and L. P. Pitaevskii, *Electrodynamics of Continuous Media* 2nd Ed., (Butterworth Heinemann, Oxford, 1995).
- [S14] L. J. Zou, D. Marcos, S. Diehl, S. Putz, J. Schmiedmayer, J. Majer, and P. Rabl, Implementation of the Dicke lattice model in hybrid quantum system arrays, *Phys. Rev. Lett.* **113**, 023603 (2014).
- [S15] J. J. Sakurai, *Modern Quantum Mechanics* (Addison-Wesley, Reading, MA, 1993).
- [S16] A. Lenef, S. W. Brown, D. A. Redman, and S. C. Rand, Electronic structure of the N-V center in diamond: Experiments, *Phys. Rev. B* **53**, 13427 (1996).
- [S17] V. M. Acosta, Optical magnetometry with nitrogen-vacancy centers in diamond, Ph.D. thesis, University of California, Berkeley, 2011.
- [S18] H. D. Young, *University Physics* 7th Ed., (Addison Wesley, San Francisco, 1992).
- [S19] P. A. Belov, Backward waves and negative refraction in uniaxial dielectrics with negative dielectric permittivity along the anisotropy axis, *Microw. Opt. Technol. Lett.* **37**, 259 (2003).

- [S20] A. Jarmola, V. M. Acosta, K. Jensen, S. Chemerisov, and D. Budker, Temperature- and magnetic-field-dependent longitudinal spin relaxation in nitrogen-vacancy ensembles in diamond, *Phys. Rev. Lett.* **108**, 197601 (2012).